PHYSICAL REVIEW B VOLUME 18, NUMBER 4 15 AUGUST 1978

Photoelectron spectra of transition-metal carbonyl complexes: comparison with the spectra of adsorbed CO

E. W. Plummer
Department of Physics and Laboratory for Research on the Structure of Matter, University of Pennsylvania, Philadelphia, Pennsylvania 19104

W. R. Salaneck and J. S. Miller
Xerox Webster Research Center, Webster, New York 14580

(Received 27 January 1978)

The uv and x-ray photoelectron spectra of carbon monoxide and transition-metal (TM) carbonyl complexes have been studied. The systematic changes in these spectra were recorded as the number of metal atoms in the complexes was increased and as the bonding configuration of the CO changed. The observations on TM carbonyl complexes are compared to the spectra of CO adsorbed on corresponding TM surfaces. We show this comparison for the electron binding energies, the shake-up spectra, the relative peak intensities, and the Auger-peak kinetic energies, as a function of the number of metal atoms in the TM carbonyl complexes. A single-metal-atom carbonyl complex reproduces nearly all of the features of the photoelectron spectra of adsorbed CO. However, there are subtle features of the photoelectron spectra of adsorbed CO, associated with molecular orbitals of CO which participate in the bonding to the substrates, which can only be reproduced by multimetal carbonyl complexes. Three or four metal atoms in a carbonyl complex are sufficient to reproduce the spectra associated with CO adsorbed on the corresponding semi-infinite TM solid.

I. INTRODUCTION

Photoelectron spectroscopy has become widely used as a technique to study molecular adsorption phenomena on solid surfaces. In nearly every case where the technique has been successful the interpretation has been based upon a comparison of the photoelectron spectra of the adsorbed molecule to that of an appropriate molecule in the gas phase. In this paper, we present the results of a study of the photoelectron spectra of the transition metal (TM) carbonyl complexes. These molecules have been chosen because they allow us to study the photoelectron spectra both as a function of the number of metal atoms and as a function of the bonding configuration of the CO molecules. In an attempt to delineate the characteristics of adsorbed and bonded CO, the spectra from the TM carbonyl complexes are compared to the spectra obtained when CO is molecularly adsorbed upon a TM surface.

Muetterties[1] has pointed out the potential similarities between the homogeneous chemistry of organometallic clusters and the heterogeneous chemistry of a TM surface. This implies that an understanding of the TM complexes can be a direct step to understanding surfaces. While we will only address ourselves to the static situation, as reflected in the photoelectron spectra, this similarity is not necessarily restricted to these properties. Figure 1(a) illustrates schematically two bonding configurations of molecular CO adsorbed on a TM surface. There are obviously many more hypothetical possibilities where the bond is shared among three or more metal atoms or where the molecule is canted with respect to the surface. Most of these cases are found in available TM carbonyl complexes. This paper addresses in a systematic fashion the details of the photoelectron spectra from CO bonded in such different configurations to single and multimetal TM carbonyl complexes and compares these systematics to the observed spectra of CO adsorbed on a TM surface. For example, one obvious challenge indicated by Fig. 1(a) is to try to determine from the photoelectron spectra the range of the bonding interaction when CO is adsorbed on a surface.

We have studied 13 different TM carbonyl complexes whose geometrical parameters are known and listed in Table I. Figures 1(b), 1(c), and 1(d) illustrate the different types of structure available. In Fig. 1(b) we show $W(CO)_6$ as an example of a case where all of the CO molecules are terminally bonded. When the TM molecule has metal-metal bonds there exists the possibility for dinuclear carbonyl bridge bonding which is shown for $Fe_2(CO)_9$ in Fig. 1(c); however, dinuclear bridge bonding is not mandatory, e.g., $Re_2(CO)_{10}$ has only terminally bonded CO ligands. Similarly, for the systems with a greater degree of M-M bonding, bridge bonding many or may not be present. For example, Fig. 1(d) shows $Ir_4(CO)_{12}$ which also has no bridge-bonded CO ligand. Note that the M-C-O angles listed in column V of Table I for terminally

TABLE I. Carbonyl structure. [a]

I Carbonyl	II terminally bonded CO	III Terminal *M*-C distance (Å)	IV Terminal C-O distance (Å)	V Terminal *M*-C-O angle (deg)	VI bridge bonded CO	VII Bridge *M*-C distance (Å)	VIII Bridge C-O distance (Å)	IX Bridge *M*-C-*M* angle (deg)	X *M*-*M* distance (Å)
CO	0		1.13						
$Ni(CO)_4$ [d]	4	1.82	1.15		0				
$Fe(CO)_5$	5	1.81(axial) 1.83(plane)	1.15		0				
$Cr(CP)_6$	6	1.92	1.17	180	0				
$Mo(CO)_6$	6	2.06	1.16	180	0				
$W(CO)_6$	6	2.07	1.16	180	0				
$Fe_2(CO)_9$	6	1.84	1.16	177	3	2.02	1.18	77.8	2.52
$Re_2(CO)_{10}$ [d]	10				0				3.02
$Mn(CO)_{10}$	10	1.82	1.16	177	0				
$CO_2(CO)_8$	6	1.80	1.17	176	2	1.92	1.20	23	2.52
$Fe_3(CO)_{12}$	10	1.84	1.14	173	2 [b]	2.16 [b] 1.95	1.13	76	2.68(T) 2.56(B)
$Ru_3(CO)_{12}$	12	1.91	1.14	173	0				2.85
$Os_3(CO)_{12}$	12	1.95	1.14	169	0				2.88
$Ir_4(CO)_{12}$	12	1.93							2.63
$Co_4(CO)_{12}$	9	1.87	1.03	164	3	2.06	1.16		2.48
$Rh_4(CO)_{12}$ [d]	9	1.96	1.10	165	3	1.99	1.36		2.73
$Rh_6(CO)_{16}$	12	1.86	1.16		4 [c]	2.17 [c]	1.20 [c]	79.5 [c]	2.78

[a] See Ref. 2.
[b] $Fe_3(CO)_{12}$ has two CO molecules bridged with one Fe atom in common. The *M*-C distances are different.
[c] For $Rh_6(CO)_{16}$ the bridge geometry is trinuclear.
[d] These carbonyl complexes are not investigated in this study.

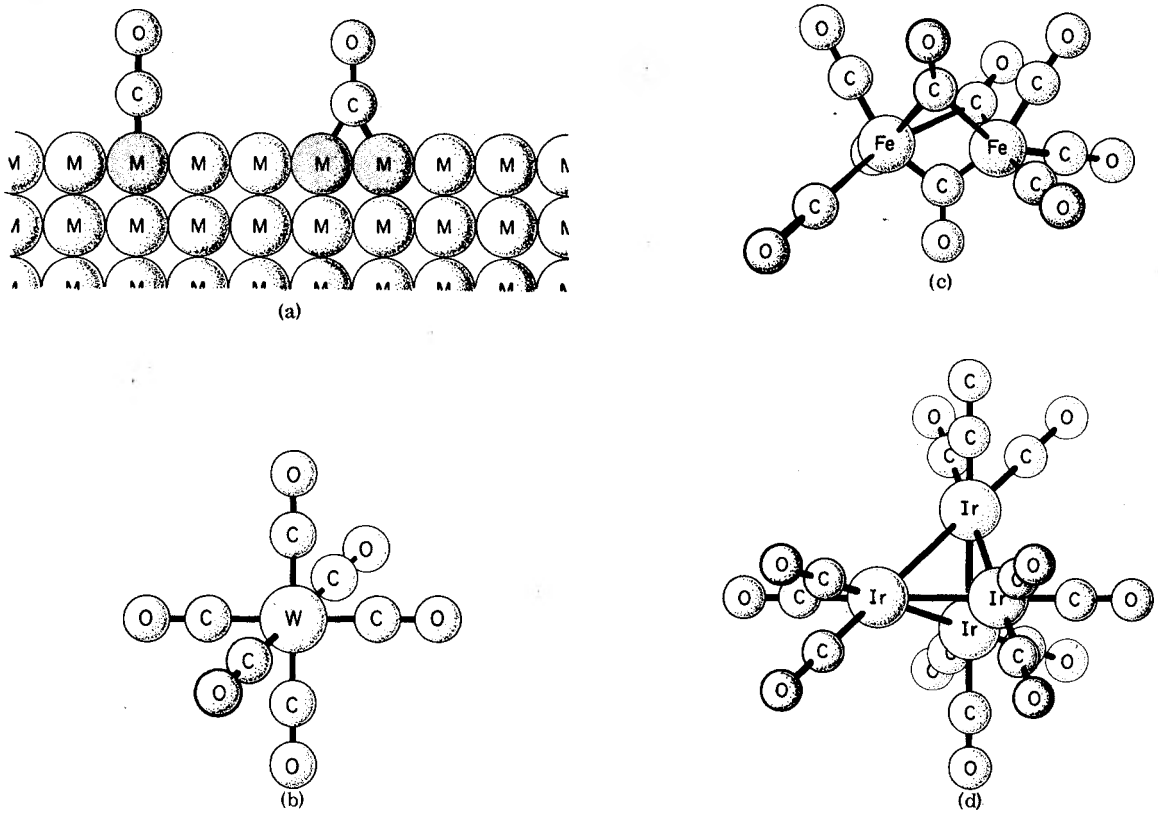

FIG. 1. Ball and stick structures of CO bound to a transition metal: (a) a solid surface with terminal and bridge-bonded CO, (b) $W(CO)_6$, (c) $Fe_2(CO)_9$ with three bridge-bonded CO molecules, and (d) $Ir_4(CO)_{12}$.

bonded CO molecules may deviate from 180°, i.e., from colinearity, by as much as 16°. Cotton and Wilkinson[3] point out that this is quite common, except when the CO molecule lies along a molecular symmetry axis of order three or higher. If this is correct, bent bonding may also occur on certain surfaces.

Through inspection of the structural parameters (Table I), several generalizations can be made. (i) Dinuclear bridge bonding usually occurs when the metal-metal spacing is less than 2.6 Å.[3] If dinuclear bridge bonding does occur for larger metal-metal spacing the C-O distance increases substantially. For example, $Rh_4(CO)_{12}$ has a metal-metal spacing of 2.73 Å and the C-O distance has increased from the equilibrium value of 1.13 to 1.36 Å. It would appear that, given the choice, CO would rather bond trinuclearly than dinuclearly when the metal-metal spacing is greater than 2.6 Å. This is the case for $Rh_6(CO)_{16}$, where the C-O spacing in the trinuclear bridge bonded CO is 1.2 Å. (ii) The metal-metal bond distances observed in the multimetal complexes is generally 2 to 4% larger than the metallic spacing (see Table V). The two exceptions are $Ir_4(CO)_{12}$ and $Co_4(CO)_{12}$.

The questions we wish to address are: (a) how do the photoelectron spectra reflect these bonding changes, and (b) how do the spectra of the TM carbonyl complexes compare with the spectra obtained from CO adsorbed on a semi-infinite TM surface? Section II describes briefly the experimental apparatus and procedure used in this work. Section III discusses in detail the features of the photoelectron spectrum obtained from a TM carbonyl complex, and Sec. IV compares the photoelectron spectrum of a TM carbonyl with that of CO adsorbed on a TM surface. General characteristics of these two types of systems, molecular complexes and surface adsorbates, will be examined. The photoelectron spectra of two surface adsorption systems, CO on Ru(001) and CO on W(110), will be compared in detail to the photoelectron spectra of the TM complexes $W(CO)_6$ and $Ru_3(CO)_{12}$. These two surface systems are chosen because a complete set of photoemission spectra have been reported by Menzel's group,[4-7] in sufficient detail to allow quantative comparison to be made with our carbonyl spectra.

II. EXPERIMENTAL APPARATUS AND PROCEDURE

The solid-phase vacuum ultraviolet photoelectron spectra (UPS) and both the vapor-phase and solid-phase x-ray photoelectron spectra (XPS) were measured on an AE1 ES 200B photoelectron spectrometer equipped with an interchangeable gas cell and a low-temperature solid probe. The base pressure of the instrument, when set up for solid-phase measurements, was $\sim 2 \times 10^{-9}$ Torr. Both Mg $K\alpha$ radiation ($\hbar\omega = 1253.7$ eV) and Al $K\alpha$ radiation ($\hbar\omega = 1486.7$ eV) were used for XPS studies. The Al anode is used with a crystal monochromator, primarily to remove x-ray satellite structure, but with some improvement in overall resolution. Vacuum ultraviolet photoelectron spectra at 21.2 and 40.8 eV were obtained for solid samples using the AE1 spectrometer equipped with a Vacuum Generators uv lamp. Vapor phase UPS was carried out on a Vacuum Generator's model UVG3 photoelectron spectrometer.

The resultant resolution for the solid-phase XPS was 0.75 eV, as measured from the Au 4*f* lines. This was primarily the limit set by the photon width of the Mg anode, with the analyzer slits closed down. The slits were opened up when the x-ray monochromator was used to increase the counting rate and maintain approximately the same resolution. The inherent width of the condensed phase carbonyl core levels was approximately 1.2 to 1.4 eV, larger than the resolution of the instrument. The low signal levels in the gas-phase x-ray measurements required the opening of the analyzer slits, which produced a full width of half maximum on the C-1s line of CO of 1.2 eV. The instrumental resolution for solid-phase UPS was ~0.1 eV.

The effective work function of the AE1 analyzer was determined for the gas-phase data by defining the binding energy for ionization from the 5σ level of CO at 14.0 eV.[8] The linearity of the sweep was checked by measuring the binding energies of the Au 4*f* levels at fixed analyzer pass energy and biasing the sample substrate with a carefully calibrated voltage source. The zero of kinetic energy (and consequently the absolute binding energies for a condensed phase carbonyl) was determined by measuring the vacuum cutoff in the UPS. The vacuum cutoff was used to measure the binding energy of the 4σ level of CO in the 40.8-eV spectrum. This value was then used to fix the absolute energy scale of the XPS data. The position of the vacuum cutoff in the UPS was in principle a function of the condensed film thickness but for the thin films which we used (20–50 Å) the measured binding energies appeared to be independent (within experimental error) of the film thickness.

The carbonyl complexes were run in the gas phase whenever possible. In most cases, however, the carbonyls did not have sufficiently high vapor pressure at temperatures below their decomposition temperature so that their spectra could be obtained in a gas-phase measurement. In these cases the carbonyl was sublimed at lower temperatures onto a clean Au surface held at a controlled low temperature. By adjusting both the temperature of the Au substrate and the pressure of the carbonyl source, the film thickness could be controlled. In a typical XPS spectrum the carbonyl film was allowed to grow in thickness until the 4*f* levels of the Au substrate were not observable in the XPS spectra, i.e., down in magnitude by $\gtrsim 10^3$ from their original intensity. This corresponds to a thickness of $\gtrsim 100$ Å. Samples less than half of this thickness were necessary for UPS measurements, to avoid sample charging effects.

We never observed x-ray induced photodissociation of the condensed-phase carbonyls when the Au substrate was precooled. Yet all of the iron carbonyl decomposed instantly on the Au surface when the substrate was near room temperature. Additionally, an O-1*s* core-level spectrum of $W(CO)_6$ condensed on a Au-cooled substrate could be run immediately upon deposition of the carbonyl and five hours later (0.2-kW x-ray power) with no observable change in binding energy or line shape, while long-running times sometimes produced an additional weak lower binding energy C-1*s* peak, which we attribute to hydrocarbon contamination from the hot x-ray gun window. This window is very close to the cold sample.

III. GENERAL CHARACTERISTICS OF CARBONYL SPECTRA

The characteristic features of the x-ray-induced photoelectron spectra of TM carbonyl complexes are illustrated in Fig. 2. In this figure the O-1*s* spectra are shown on the left and the valence spectra on the right, for gas-phase CO, gas-phase $Cr(CO)_6$, and condensed $Cr(CO)_6$. The C-1*s* spectra (not shown) are qualitatively similiar to the O-1*s* spectra. We use atomic rather than molecular notation to label these core levels in order to emphasize their physical origin. As an aid in visualizing each of the CO molecular orbitals, we have shown the wave function contour plots of Johnson and Klemperer[9] in Fig. 3. The molecule in this figure is oriented with the carbon to the left, and the letters *T* and *B* indicate the approximate position of the metal atoms in a terminal or bridge-bonding configuration, respectively. Figure 3 is a plot of the effective one-electron molecular orbitals for neutral CO, where the 1σ, 2σ,

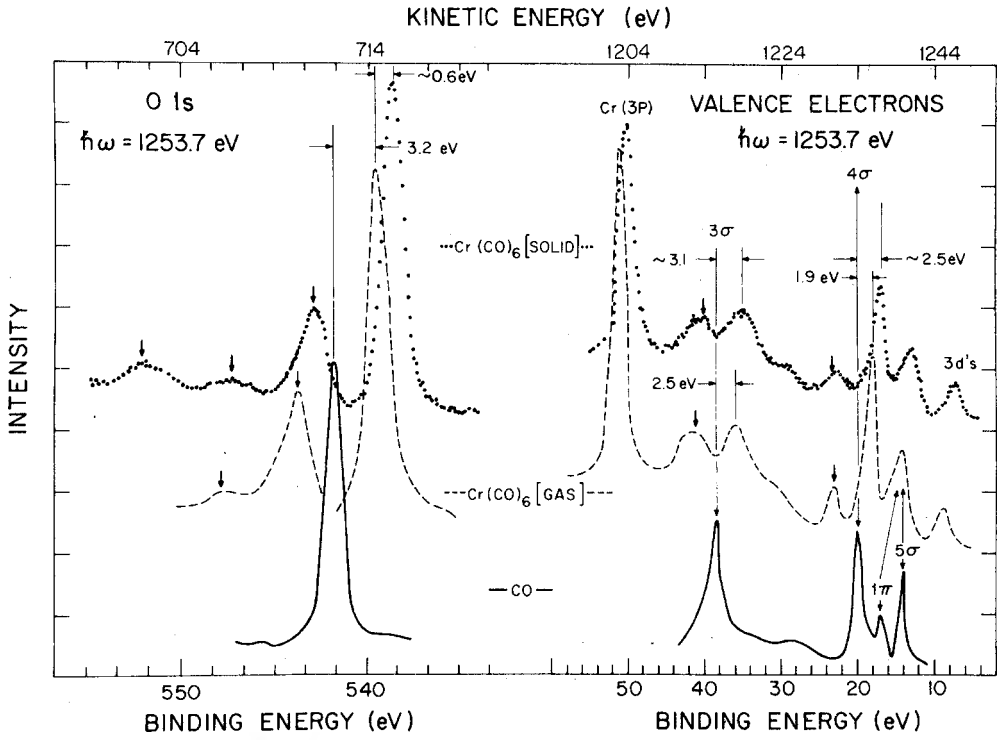

FIG. 2. Photoelectron spectra ($\hbar\omega = 1253.7$ eV) of the O-1s core region (left) and valence region (right) of gas phase CO and $Cr(CO)_6$, and condensed phase $Cr(CO)_6$. The vertical unmarked arrows indicate the observed shake-up peaks on the O-1s, CO-3σ, and CO-4σ energy levels.

3σ, 4σ, and 5σ levels are occupied by two electrons and the 1π level by four electrons. The 2π level is the first unoccupied orbital of CO. When we use this labeling in a photoelectron spectrum (Fig. 2) we mean that one electron has been photoionized from the designated neutral molecular orbital. This nomenclature is conventional and convenient, but in many cases it is misleading and confusing. The reasons that this notation can be misleading are (i) that it refers to a single-particle molecular-orbital picture, and (ii) photoelectron spectroscopy measures the energy states of the positive ion, not of the neutral.

Each peak in the photoelectron spectra shown in Fig. 2 corresponds to a different energy state of the positive ion, where the binding energy (E_B) of peak (i) is given by

$$E_B(i) = E_{\text{ion}}(i) - E_0 . \qquad (1)$$

In this equation $E_{\text{ion}}(i)$ is the total energy of the ith excited state of the positive ion and E_0 is the total energy of the neutral before photoionization. We assume that the molecule is in the ground state before excitation. The lowest energy state of the ion, which we label $i = 0$, produces a binding energy $E_B(0)$ equal to the threshold ionization potential of the molecule. For example, the lowest binding-energy peak for gas-phase CO, shown in Fig. 2, has a value of 14 eV, i.e., the ionization potential of CO is 14 eV. We have labeled this peak in Fig. 2 as the 5σ peak, where we mean that one electron has been removed from the 5σ orbital of neutral CO. All of the other peaks in the photoelectron spectrum of CO correspond to excited states of the ion (including multiple ionization). The correct notation for the peaks in a spectrum like that shown in Fig. 2 should correspond to the ionic states of the molecule. We will not use an ionic notation because we don't know the correct labeling for many of the peaks and we want to maintain a closer contact with the one-electron picture of the molecules.

The price that must be paid for using a one-electron neutral nomenclature to label the photoelectron spectra is some degree of confusion, usually resulting from insufficient information in the labeling or from the inappropriateness of a one-electron scheme. For example, even in a one-electron picture, denoting a peak in the left-hand panel of Fig. 2 as the O-1s peak does not describe the state of the ion. The O-1s notation means that these peaks (four in the condensed-phase spectra) are in

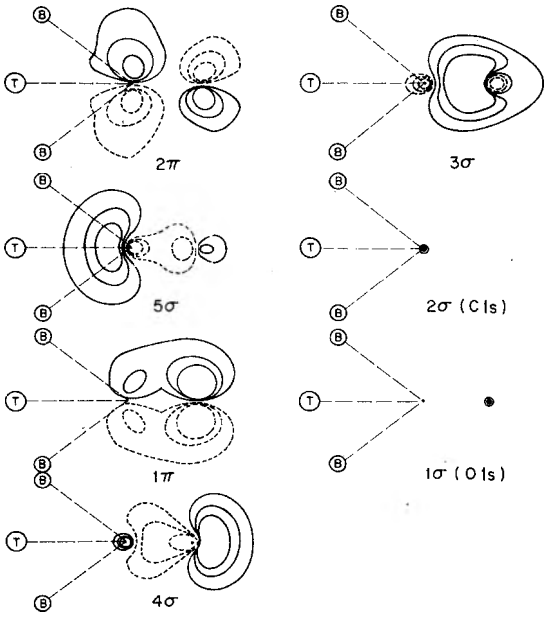

FIG. 3. Wave-function contours for the carbon monoxide molecular orbitals (Ref. 9). Solid and broken lines indicate contours of opposite sign having absolute values of 0.3, 0.2, and 0.1. The molecule is oriented with carbon on the left and oxygen on the right. The *T*'s on the figure indicate where the TM atom would be located for a terminally bonded CO and the *B*'s are for the bridge-bonded CO.

the appropriate energy range to be a state of the ion with one electron missing from the O 1*s* level, but does *not specify* the distribution of the remaining electrons in the molecular ion. The peak with the lowest binding energy in the O-1*s* region of Fig. 2 is the lowest total-energy configuration of $Cr(CO)_6$ singly ionized with one electron missing from an O 1*s* level of one of the six oxygen atoms. The molecular orbitals of this state of the ion will look quite different from the molecular orbitals of the neutral molecule (Fig. 3) and the occupancy of the remaining energy levels may be different. We have belabored this point here because it will be essential later to understand the detailed picture in the photoelectron spectra of the carbonyls.

We will discuss various portions of the photoelectron spectra of TM carbonyl complexes. The three most obvious differences between the gas-phase spectrum of CO and the spectrum of a carbonyl can be seen in Fig. 2. (a) There are satellite structures (indicated by the vertical unmarked arrows) on the low kinetic energy side of the most intense lines of each CO-derived peak, labeled via our neutral nomenclature. These peaks are called shake-up peaks. (b) The main peak (most intense and lowest binding energy) associated with each CO level is shifted to a lower binding energy in the carbonyl spectrum. For example, the gas-phase peak with the lowest binding energy in the O-1*s* region of the $Cr(CO)_6$ spectrum is shifted approximately 3 eV from the O-1*s* peak in gas-phase CO. (c) There is a differential energy shift of the CO 1π and the CO 5σ orbitals, which causes them to appear degenerate in the carbonyl photoelectron spectra. The 5σ orbital as explained below is the orbital primarily involved in the bonding of the CO to the TM. One additional feature of the photoelectron spectra of CO and of the carbonyls will be discussed, namely, the Auger spectrum. The Auger spectrum results from processes involving two electrons, one filling either the O-1*s* or C-1*s* hole created by photoionization and the second being ejected leaving the molecule in a doubly ionized state.

Before discussing the features mentioned above, we will give a brief review of a model for bonding of CO to a TM atom. The traditional view of this bond has been a synergic model where σ donation to the metal from the 5σ CO orbital is accompanied by metal-to-π back donation into the CO 2π unoccupied orbital (Fig. 3).[3,9] It was originally thought that both the 5σ and 2π orbitals of CO were antibonding, and consequently when charge transfer out of the 5σ occurred upon σ donation, back donation into the 2π was required to maintain the observed small change in the CO dipole moment and vibrational frequency. In contrast to this notion, a recent calculation by Johnson and Klemperer[9] for $Cr(CO)_6$ indicates that the bonding is predominantly σ in character with only a small π contribution. This is possible because the CO 5σ orbital (Fig. 3) is a nonbonding orbital which protrudes out of the carbon end of the molecule. The role of back bonding into the 2π level of CO is still not resolved.[10,11] Yet all calculations indicate that the occupied 5σ and unoccupied 2π are the only two molecular orbitals of CO which participate in the bonding to a TM atom.[10,11]

The following sections will describe the behavior of the shake-up energies (A), the shake-up intensities (B), the one-electron binding energies (C), the 5σ bonding orbital (D), and the Auger spectra (F) as a function of the number of metal atoms in the complex. In principal we should discuss how these spectra were effected when the CO bonding changed from terminal to bridge. In practice very little change was observed. These results are discussed in Sec. III E.

A. Shake-up energies

We begin our discussion of the carbonyl spectra with the satellite structure associated with every

CO-derived peak. This satellite structure on the low kinetic energy (high binding-energy) side of the most intense peak is commonly referred to as the shake-up spectrum.[12] The term shake up implies that the outer valence electrons of the molecule have been excited in the process of photoionization, leaving the ion in a higher energy state, i.e., higher binding energy [Eq. (1)]. The most intense shake-up peak associated with the O 1*s* level in $Cr(CO)_6$ is displaced by 5.4 eV toward higher binding energy (lower kinetic energy). This means that there is a 5.4-eV excited state of the $Cr(CO)_6$ ion with one electron missing in the O 1*s* level of one of the six oxygen atoms. This shake-up peak has been reported for both the core levels and valence levels of carbonyls.[13] It is a general feature of all carbonyl spectra. Therefore, it is important to understand the configuration of the ion which is associated with both the main peak (most intense and lowest binding energy) and with the shake-up peak (or peaks).

The origin of the main peak and of the first and most intense shake-up peak can be understood by considering the following hypothetical experiments. Consider one Cr atom and one CO ligand as the basic molecular entity and examine the photoionization from the C 1*s* level of CO. The binding energy of the C 1*s* level of CO is 269.2 eV when the Cr atom and the CO molecule are placed at an infinite separation. Since the Cr atom and the Co molecule do not interact this is clearly the only peak observed in the C-1*s* region of the photoelectron spectrum, ignoring any of the relatively weak inherent shake-up peaks for an isolated CO molecule. But this ionic state is not the lowest energy state of the CO-Cr system with a C-1*s* hole. This can easily be seen by removing an electron from the Cr atom and placing it in a lower energy state on the positive CO ion. The energy required to remove this electron from the Cr atom is 6.7 eV for the $3d^5 4s^1$ configuration and 6.3 eV for the $3d^6$ configuration.[14] The ionized CO molecule with an electron missing in the C 1*s* level looks just like the NO with the CO spacing, so the energy gained when the electron is placed in the 2π orbital of NO is 9.2 eV.[8] Therefore, the ionic configuration corresponding to neutral CO in an excited state and singly ionized Cr is 2.5–3.0 eV lower in energy than the original ionic state.

Figure 4(a) is a schematic energy-level diagram for the neutral metal plus CO system on the left and the two configurations of the molecular ion on the right. The case when one electron is photoionized from the C 1*s* level (2σ), the lowest energy configuration of the ion with this hole, is shown in the first diagram on the right. The C-1*s* hole is screened by charge transfer from the metal *d* levels to the highest unoccupied molecular orbital of the positive CO ion, i.e., the 2π. The energy diagram on the far right shows an excited state of the ion where there has been no charge transfer from the metal. This simple picture shows that in terms of the spectroscopic notation of the ground-state configuration of the neutral metal atom plus CO molecule that the lowest energy configuration of the ion with a C 1*s* electron missing is a two-hole state, one hole in the C 1*s* level and the other in the metal *d* level. The CO, on the other hand, is in an excited state of the neutral molecule, with the C-1*s* electron excited to the 2π level.

We have tried to illustrate schematically in Fig. 4(b) what the photoelectron spectra from the C 1*s* level will look like as the CO molecule is brought in from infinity. When the carbon-metal spacing is infinite only one peak will be observed. This will be the gas-phase CO, C-1*s* peak at 296.2 eV. There is a lower energy state of the system but it requires the transfer of charge from the metal to the CO, which will not occur when the metal is far away. Therefore, the intensity in the spectrum will be zero in this state. Curve (*a*) of Fig. 4(b) depicts this case. The two dashed lines are the energies of the two ionic states for the isolated Cr atom and CO molecule. The lowest energy state is indicated by CO*, which is the notation of Fig. 4(a). As the CO molecule is brought in closer to the metal, a finite probability for charge transfer exists upon photoionization of a C-1*s* electron. Curve (*b*) shows a hypothetical case where the spacing of the CO from the metal is larger than the 1.92-Å carbonyl distance. As the CO is moved closer to the metal atom the picture cannot remain as simple as it was at infinity. Instead of having molecular orbitals centered primarily on the CO (or atomic orbitals on the Cr), there will be molecular orbitals spread out over the entire carbonyl molecule. Yet the basic concept must be correct. The lowest binding-energy peak which requires charge transfer from the metal to the CO molecule will become stronger as the CO interacts more strongly with the metal (the probability of the transfer of an electron increases). Consequently, the second peak which originally corresponded to an ionized CO molecule will decrease in intensity. Curves *c*, *d*, and *e* of Fig. 4(b) depict what could happen as the spacing is decreased. Curve *d* is from our measurements for $Cr(CO)_6$ where the intensity of the higher binding-energy peak. Curve *e* represents a 0.05 Å decrease in the Cr-C spacing with a resultant decrease in intensity to 17%. This was estimated from the work of Barber *et al.*[13] on the decrease in intensity of the O-1*s* shake up with decreasing metal-carbon spacing. The details of the intensities and energy separation be-

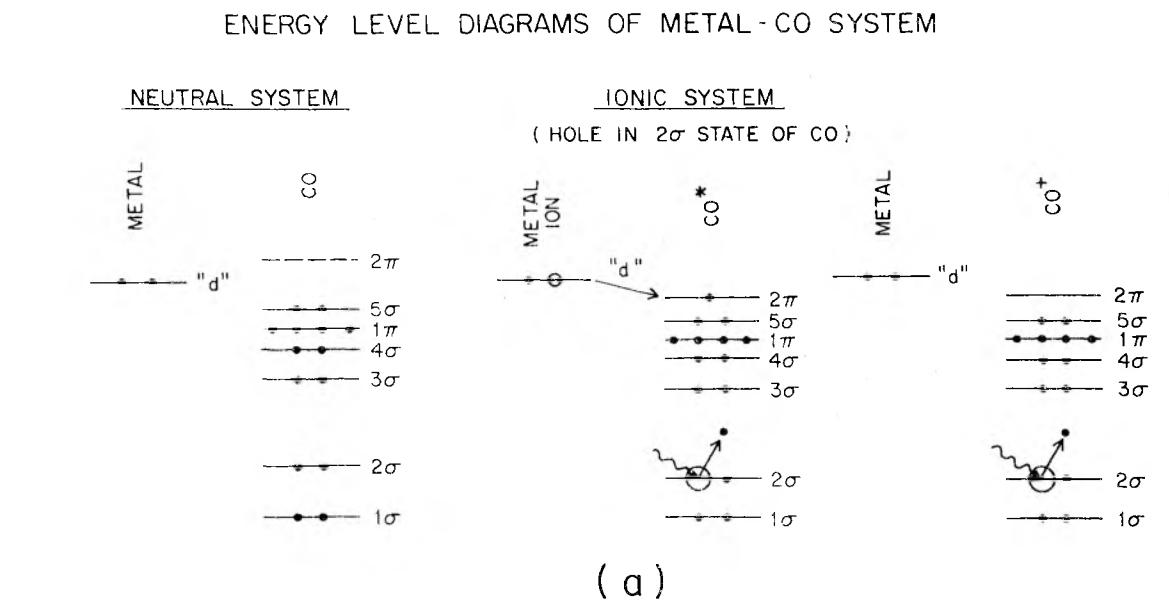

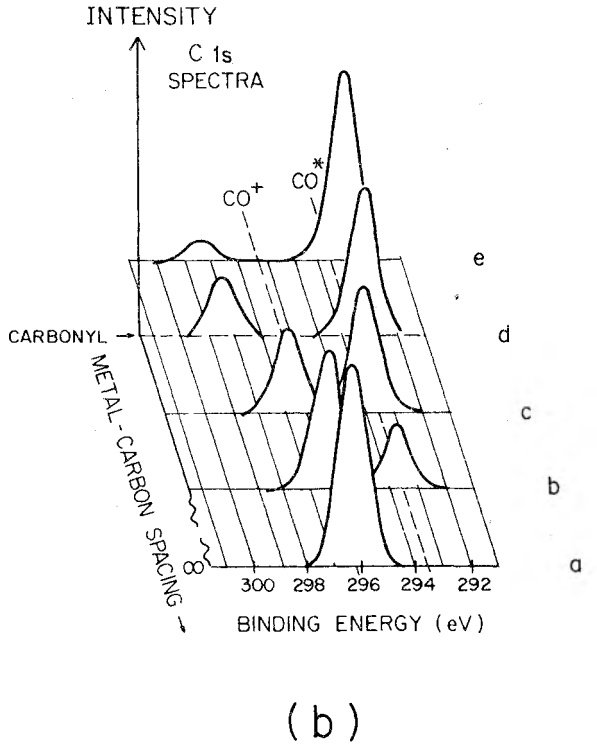

FIG. 4. (a) Schematic energy-level diagram of the neutral metal-CO system (left) and two ionic states (right) with a single 2σ hole. (b) Schematic drawing of the C-1s photoelectron spectra from a CO molecule as a function of the metal-carbon distance in a carbonyl. Curve *a* is for a CO molecule at infinity and curve *d* is the measured spectrum for $Cr(CO)_6$.

tween these peaks will depend upon the dynamics of the many-body photoexcitation process.[15] The only general statement that can be made is that the peak which is associated with the lowest energy state of a C-1s hole will decrease in binding energy as the molecule is formed. The second peak could either increase or decrease in binding energy. Experimentally this peak increases in binding energy.

The origin of the C-1s satellite was easy to visualize because a CO molecule with a hole in the C 1s level looks electronically like NO. Photoionization from the other energy levels of CO does not produce an ionic specie which can so easily be modeled by a known molecule. But we would expect

that this picture of the screening process will apply to all of the CO energy levels, except perhaps the outer most valence orbitals. This picture is the same as the "excited atom" model described previously by Lang and Williams for the photoelectron spectra (of a core level) of an atom adsorbed on the surface of free-electron-like metal.[16] The metal screens the hole created by photoionization by transferring charge to the highest unoccupied orbital of the ion, so that the adsorbed atom or molecule is in an excited neutral state [Fig. 4(a)].

If this model for the shake up is correct, it predicts, in the simplest case of no initial-state chemical shift, that as the size of the molecule increases by adding more metal atoms, the separation between the main core-level peak (lowest binding energy) and the first satellite should increase. This is a consequence of lowering the energy of the ion by delocalizing the hole.[16] In contrast the energy of the first shake-up peak of a neutral metal and ionic CO should not be changed much as the number of metal atoms increases, since the polarization field from the CO ion is short ranged. We know experimentally that when CO is molecularly adsorbed on W(110) and Ru(001) that the shake-up energy on the O 1s energy level is ~7 eV for both cases.[7] This value gives us the limit for an infinite number of metal atoms in a cluster. One must be a little careful with this comparison because the energy of the shake up will change if the bonding energy of CO with the metal changes substantially [see Fig. 4(b)].

In Fig. 5 the energy of separation of the O-1s shake-up peak from the main O-1s peak as a function of the number of metal atoms in the carbonyl complex is plotted. In general, the shake-up energy increases with the number of metal atoms and apparently saturates at approximately 7 eV for four metal atoms in the cluster. This increase in the shake-up energy with an increasing number of metal atoms is consistent with our model of this excitation, since the bigger molecules have a more delocalized metallic hole. Therefore, the change shown in Fig. 5 in going from a single metal carbonyl complex like $W(CO)_6$ to a multimetal carbonyl like $Ru_3(CO)_{12}$ is not a consequence of any change in the bonding of CO, but instead reflects changes in the excitation spectra of the ion caused by the delocalization of the wave function over the metal atoms. Note in Fig. 5 that the shake-up energy for $Fe_3(CO)_{12}$ is abnormally low for a three-metal-atom carbonyl. This carbonyl will consistently display spectra indicative of a single- or double-metal carbonyl complex.

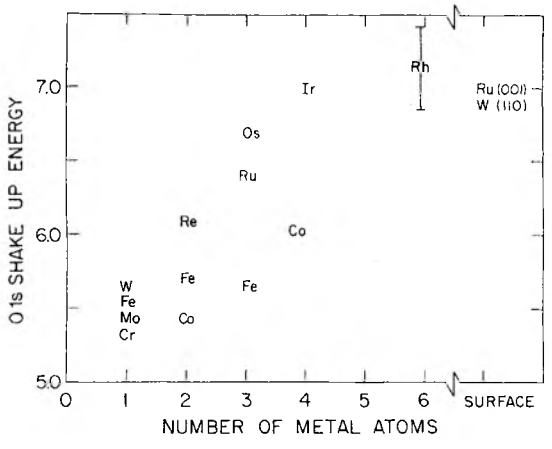

FIG. 5. Plot of the energy separation between the O-1s peak and the most intense shake-up peak in the photoelectron spectra of TM carbonyls (condensed), as a function of the number of metal atoms in the carbonyl. The data points are indicated by the chemical letters identifying the metal atoms (Table I).

B. Shake-up intensities

The origin of the intensity variation in the satellite structure can be visualized through the aid of a model invoking the sudden approximation. In this model we picture the photoionization process being so fast that the $N-1$ remaining electrons are caught "frozen" in their respective neutral orbitals. This state is not an eigenstate of the ionic Hamiltonian. The intensity of each satellite peak is given by the projection of this $N-1$ "frozen" wave function onto the true states of the ion. This picture is very analogous to the Franck-Condon principle for electronic transitions in a vibrating molecule.[17] After an electronic transition the old vibrational wave functions of the neutral molecule are not eigenstates of the new Hamiltonian of the ion. The probability of ending up in a given vibrational state of the new electronic state is given by the square of the overlap of the vibrational wave functions of the old and new Hamiltonians.

If $\psi_F^{N-1}(i)$ is the frozen orbital wave function of the N-1 system with an electron removed from the ith orbital and $\psi_k(i)$ is the wave function for the ionic Hamiltonian in the kth state, then the probability of observing the kth state of the ion is

$$P_{ki} \propto \left| \langle \psi_F^{N-1}(i) \, | \, \psi_k(i) \rangle \right|^2 .$$

If $k=0$ denotes the lowest energy state of the ion with an electron missing from the ith orbital, then we can again make the analogy with the Franck-Condon principle. The binding energy given by Eq. (1) for the $k=0$ ionic state corresponds to the adiabatic ionization potential. Likewise, the energy weighted average of all possible binding energies

corresponding to the different ionic states k will give the vertical ionization potential

$$E_v(i) = \sum_{k=0} P_{ki} E_B(i,k) , \qquad (2)$$

where $E_v(i)$ denotes the vertical ionization potential and $E_B(i,k)$ is the binding energy of each state of the ion k with a hole in the ith orbital. Lundqvist,[18] and Manne and Åberg[17] have shown within different theoretical approximations that this first moment of the spectra can be related to the properties of the electron in the ith orbital of the neutral molecule. Manne and Åberg[17] proved that the energy $E_v(i)$ is the Koopmans' theorem binding energy within a Hartree-Fock scheme. Lundqvist[18] calculated $E_v(i)$ for core excitation with electron-plasmon coupling. He showed that the difference between $E_B(i,0)$ and $E_v(i)$ was the polarization energy. In both of these models, the difference between $E_v(i)$ and $E_B(i,0)$ should be the relaxation energy of the ion from its "frozen-orbital" configuration. In principle, the change in $E_v(i)$ as an atom bonds in different environments reflects directly the chemical shift of the initial state.

The difference between the first moment of the spectra $E_v(i)$ and the lowest binding-energy state $E_B(i,0)$ [Eq. (2)] can be illustrated using the data given in Appendixes A, B, and C, for the O 1s level of $Mo(CO)_6$. We use this carbonyl because the spectra for the satellite structure is the most complete that we have recorded (Appendix C). First consider the binding energy E_B (O 1s, 0) of the dominant peak shown in Fig. 2. The value for gas-phase CO is 542.6 eV, while the corresponding numbers for gas- and condensed-phase $Mo(CO)_6$ are 539.5 and 538.0 eV, respectively. This yields a reduction in binding energy of 3.1 eV between gas-phase CO and gas-phase $Mo(CO)_6$ and an additional 1.5 eV reduction when $Mo(CO)_6$ is condensed. The satellite structure on the O 1s level of CO is very small so let us take 542.6 as E_v for gas-phase CO. The first moment calculated from the data in the Appendixes for gas-phase $Mo(CO)_6$ is 541.3 eV, and 541.6 eV for condensed-phase $Mo(CO)_6$. Within the experimental accuracy of measuring and finding all of the satellite structures, these three numbers are identical. Consequently we must conclude: (i) The reduction in the O-1s binding energy is primarily a result of the final-state relaxation effects, or that there is very little chemical shift in the initial state. This was predicted theoretically for $Cr(CO)_6$ by Baerends and Ros.[19] (ii) The polarization energy shift of 1.5 eV between gas- and condensed-phase $Mo(CO)_6$ is completely compensated for by the ~16-eV satellite structure (Fig. 2; Appendix C). This large energy excitation could be some form of a collective excitation.

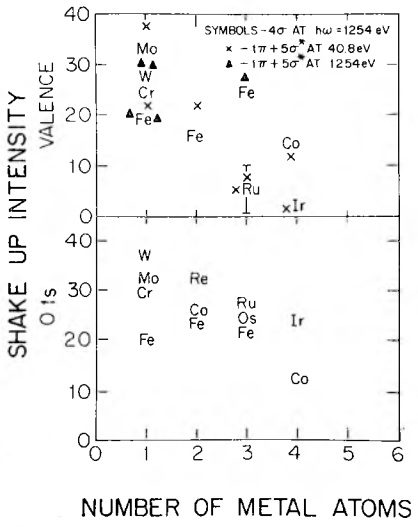

FIG. 6. Shake-up intensity for the ~6-eV shake-up peak in the carbonyls as a function of the number of metal atoms in the carbonyl complex. The bottom is for the O-1s shake up. The top is for the shake-up intensity on the valence orbitals.

There are several general features of the shake-up structure common to all TM carbonyls: (i) The intensity of the dominant satellite is larger for the C 1s level than for the O 1s level (Appendix C). (ii) The energy deficit for the first satellite is smaller for the 4σ level than for either of the core levels (O 1s and C 1s). (iii) There is a quite different variation in the intensity of the satellite on the 4σ level compared to the core levels as the number of metal atoms in the carbonyl is changed. This behavior is shown in Fig. 6. The bottom panel shows that there is a small variation in the O-1s shake-up intensity with the number of metal atoms in the complex. The top panel clearly reveals a general decrease in the satellite intensity for the valence orbitals as the number of metal atoms increases or as Fig. 5 shows, as the shake-up energy increases. Section III C will show that this effect is not accompanied by any differential shift in the relative binding energy of the O 1s level compared to the 4σ level.

C. One-electron binding energies

In this section we will discuss the changes in the binding energies of the CO-derived orbitals when CO is terminally bound in a carbonyl complex. These effects are all illustrated for $Cr(CO)_6$ in Fig. 2 and we will use this carbonyl to illustrate the general features. In this section we will only discuss the binding energy of the lowest energy ionic state of each hole configuration, which is $E_B(i,0)$ in the nomenclature used in Eq. (2).

TABLE II. Binding energies.

Level	I CO (eV)	II Gas-phase $Cr(CO)_6$ (eV)	III ΔE I − II (eV)	IV Solid $Cr(CO)_6$ (eV)	V ΔE II − IV (eV)
1σ (O 1*s*)	542.6 ± 0.1	539.4 ± 0.1	3.2 ± 0.1	538.8 ± 0.1	0.6 ± 0.2
2σ (C 1*s*)	296.2	293.1 ± 0.1	3.1 ± 0.1	292.4 ± 0.1	0.7 ± 0.2
3σ	38.3 ± 0.3	35.8 ± 0.2	2.5 ± 0.3	35.2 ± 0.3	0.6
4σ	19.7	17.8	1.9	17.2	0.6 ± 0.1
1π	16.8	14.8 ± 0.1 [a]	2.0 ± 0.2 [a]	14.2 [a]	0.6 ± 0.1 [a]
5σ	14.0	13.9	~0	13.2	0.7 ± 0.2
3*d*		8.5 [a]		7.8 [a]	0.7 [a]
3*p*		51.1		50.6	0.5

[a] Data taken with $\hbar\omega = 40.8$ eV; all other data $\hbar\omega = 1254$ eV.

Table II lists the binding energies for CO, gas-phase $Cr(CO)_6$, and condensed-phase $Cr(CO)_6$. The general features displayed in this table are characteristic of all carbonyl complexes studied in both the gas and condensed phases (Appendixes A and B). Column III of Table II lists the reduction in binding energy between gas-phase $Cr(CO)_6$ and CO. There is a nonuniform shift, with the deeper and more localized O 1*s* and C 1*s* levels (Fig. 3) experiencing a upward shift toward lower binding energies. This is consistent with the notion that the more delocalized the molecular orbital, the smaller the relaxation energy. Bagus and Hermann[20] have calculated the binding energies of the CO-derived orbitals for CO bound to one (two) Ni atoms. Their Hartree-Fock ΔSCF calculation [the threshold energy is taken as the difference in total energies of two self-consistent-field (SCF) calculations] predicted a 1.1 eV (1.5 eV) relaxation shift for the 1σ state (O 1*s*), 1.3 eV (1.7 eV) for the 2σ (C 1*s*), 0.9 eV (1.2 eV) for the 3σ, and 0.1 eV (0.3 eV) for the 4σ state. The observed values are larger, but the differential effects and trends are similar to those found theoretically.

The 5σ level, which is responsible for the bonding, appears not to be shifting. This is an accidental cancellation of a large bonding shift with an equally large relaxation shift.[20] Baerends and

TABLE III. Comparison of theory and experiment for $Cr(CO)_6$ binding energies.

I Level	II Experimental (eV)	III H-F LCAO [c] Koopmans (eV)	IV SCF [d] $X\alpha$-MSW (eV)	V HFS-DV [e] $X\alpha$ (eV)
1σ (O 1*s*)	539.4	555.2		CO −3.7 [g]
2σ (C 1*s*)	293.1	309.1		CO −3.3 [g]
3*p*	51.1	62.9		50.1 [f]
3σ	35.8	42.6		35.4 [f]
4σ	17.8	22.9	17.9	18.3 [f] / 16.4
1π	14.8 [b]	18.9	13.2	14.9
5σ [a]	13.9	18.0	13.1	13.5
3*d*	8.5	10.7	8.6	8.9

[a] 5σ denotes orbitals in $Cr(CO)_6$ originating from 5σ level of CO, when there are multiple levels. The number in the table is the weighted mean (by occupancy).

[b] Data at $\hbar\omega = 40.8$ eV.

[c] Hartree-Fock calculation using Koopman's theorem (Ref. 21).

[d] SCF-$X\alpha$ multiple-scattered-wave calculation using transition state concept (Ref. 9).

[e] Hartree-Fock-Slater discrete-variation $X\alpha$ calculation using the transition state concept (Ref. 22).

[f] Symmetry of molecule reduced in order to localize the hole (Ref. 22).

[g] The binding energy change of the O 1*s* and C 1*s* levels in the $Cr(CO)_6$ with respect to CO was reported.

Ros[19] have calculated the reduction in the O-1s and C-1s binding energies for $Cr(CO)_6$ relative to free CO. Their theoretical values are 3.7 and 3.3 eV, respectively. Table II, column III, shows that the measured values are 3.2 and 3.1 eV, respectively. In the condensed phase all of the levels exhibited an additional uniform shift due to dielectric screening of the hole by the surrounding carbonyl molecules. This fact is illustrated in the last column in Table II.

Table III compares the measured binding energies for gas-phase $Cr(CO)_6$ with three different calculations. Column III is the Hartree-Fock calculation by Hillier and Saunders[21] using Koopmans' theorem. Column IV is the SCF-$X\alpha$ scattered-wave calculation of Johnson and Klemperer,[9] where the binding energies were obtained using the transition-state concept. The final column lists the values obtained by Baerends and Ros[22] using the discrete variational $X\alpha$ calculation approach with a transition-state potential. They report only the shifts in the O 1s and C 1s levels from the original CO values. The numbers in column V indicated by the superscript (f) were calculated by breaking the symmetry of the molecule in order to localize the hole.

It is obvious from column III that Koopman's theorem produces binding energies which are too large. This is what one would expect from Eq. (1), because the ion in this scheme is not allowed to relax around the hole. Both of the $X\alpha$ techniques give very reasonable answers when compared to the experimental data. The discrete variational method gives better agreement for the separation between the 5σ and 1π orbitals. The scattered wave with its muffin tins has problems with π levels.

In Appendixes A and B the measured binding energies for gas-phase and condensed-phase carbonyls are tabulated. There are many similarities in the spectra from these molecules. For example, the difference between the O-1s and C-1s binding energies is 246.2 eV with a standard deviation of 0.18 eV. This should be compared to the value of 246.4 eV for gas-phase CO. Therefore, within experimental error the C-1s to O-1s spacing is the same in the carbonyl as it is in the gas-phase CO molecule. The calculation by Ellis *et al.*[23] for $Cr(CO)_6$ and $Fe(CO)_5$ showed that the reduction in the O-1s binding energy should be 0.3 to 0.4 eV larger than the C-1s reduction. Another binding-energy difference which appears to be independent of the details of the carbonyl is the energy between the O 1s and 4σ levels. This value is 521.4 eV with a standard deviation of 0.2 eV. The gas-phase CO value is 522.9 eV. This difference of 1.5 eV between CO and the carbonyl is the differential energy shift shown in Fig. 2. The separation between the 4σ and 3σ levels in the carbonyls is 17.8 ± 0.3 eV with $Ir_4(CO)_{12}$ having the smallest spacing observed (17.1 eV). This number should be compared to ~18.6 eV separation for CO in the gas phase.

There are three features of the one-electron spectra which do depend upon the nature of the carbonyl complex, the bonding 5σ orbital, the metal energy levels and the splitting of core levels due to bridge bonding.

D. $5\sigma^*$ bonding orbital

We will always use the $*$ on the 5σ orbital to denote the orbital or orbitals in the carbonyl which are primarily derived from the CO 5σ orbital. Figure 2 showed that this energy level becomes nearly degenerate with the CO 1π energy level when CO is bound to a metal atom in a carbonyl. All of the theoretical calculations on $Cr(CO)_6$ show that the molecular orbitals derived from the 5σ overlap those derived from the 1π.[9,21,22] Therefore, it is difficult if not impossible to resolve these energy levels in a photoelectron spectrum, independent of the resolution. We have attempted to separate the 1π and $5\sigma^*$ levels in the photoelectron spectra of the carbonyls by using the variation in the cross sections of these two levels with photon energy. In a UPS spectrum[8] of CO the 1π has the largest cross section, while Fig. 2 shows that in the x-ray induced spectrum the 5σ is larger than the 1π. This behavior is a consequence of the 2s character of a σ state compared to the 2p character of the 1π state. Figure 7 displays the difference between a valence-band spectrum obtained with $\hbar\omega = 40.8$ and 1254 eV, where the curves have

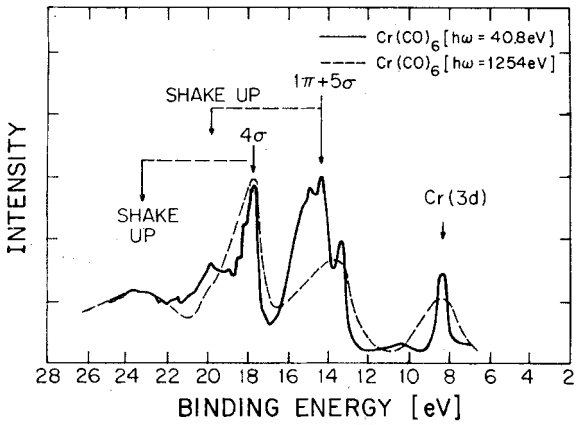

FIG. 7. Comparison of the gas phase $Cr(CO)_6$ valence-band spectrum taken at $\hbar\omega = 40.8$ eV with the spectrum obtained using $\hbar\omega = 1254$ eV.

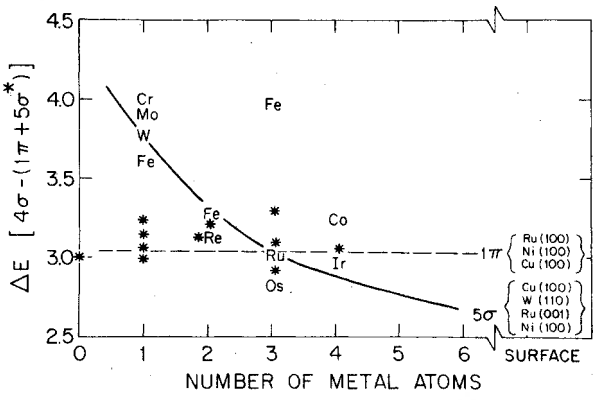

FIG. 8. Binding energy separation between the CO 4σ level and composite 1π+5σ* level of the carbonyl as a function of the number of metal atoms in the carbonyl complex. The *'s are data points taken at $\hbar\omega = 40.8$ eV, while the symbols are for excitation with x rays. The notation on the right is for the determination of the 4σ to 5σ* or to 1π spacing for CO adsorbed on single crystals (Refs. 5, 33 and 34).

been normalized at the peak intensity in the 4σ level. It is obvious, even with the lower resolution in the x-ray spectrum, that the centroid of the 1π + 5σ* level has moved to lower binding energy in the x-ray spectrum compared to the uv spectrum. The energy spacing between the 4σ and the centroid of the 1π + 5σ* levels has increased from 3.1 eV in the 40.8-eV spectrum to 4.0 eV in the x-ray spectrum. We will use the low-photon-energy spectrum to obtain the 4σ to 1π spacing and the x-ray spectrum to give us the 4σ to 5σ* energy spacing in the carbonyls.

Figure 8 is a plot of energy spacing between the CO 4σ level and the combined 1π + 5σ* level as a function of the number of metal atoms in the carbonyl complex. The chemical symbols are the measurements made with x-ray excitation and the * symbol is the energy spacing measured at 40.8 eV. According to the argument given above the *'s represent the 4σ to 1π energy spacing, which as shown in the figure is relatively independent of the number of metal atoms in the complex. The 4σ to 1π spacing is about 3.1 eV in the carbonyls, slightly larger than the equivalent spacing in the isolated CO molecule. The x-ray data, on the other hand, show that the 4σ to 5σ* energy spacing decreases as the number of metal atoms in the complex increases. The data points on the right are measurements made on CO adsorbed on different single-crystal surfaces.

The ~1.5-eV relative shift in the 5σ* binding energy with respect to the 4σ binding energy between a single-metal atom carbonyl and a large multimetal atom carbonyl complex or a surface does not result from changes in the binding of CO in the complexes. It must be a consequence of the variation in the relative relaxation energy associated with the two orbitals as the size of the cluster increases. Ellis *et al.*[23] have shown that the relaxation energy for the 5σ orbital in a $(Ni)_5CO$ cluster is 0.9 less than the corresponding relaxation energy for the 4σ orbital. Yet Bagus and Hermann[20] found that the relative relaxation shift was opposite in a NiCO calculation, 0.5 eV greater for the 5σ than for the 4σ. Therefore, a plausible explanation of the data shown in Fig. 8 is that the differential relaxation energy between the 5σ* and 4σ energy levels changes as the molecular complex increases in size. If this argument is correct, than the argument given for the change in the core-level shake-up energy in Sec. IIIC is nearly similar and there should be a direct correlation between the shake-up energy on a core level and the energy separation between the 4σ and 5σ* energy levels. This plot is shown in Fig. 9. There is almost a one-to-one correlation between the shake-up energy and the valence-orbital-energy spacing. Even the $Fe_3(CO)_{12}$ complex which appeared as an abnormal point on Figs. 5 and 8 falls on the straight line. Evidently, the relaxation energy of the more localized CO molecular orbitals like the 4σ increases more rapidly as the cluster size increases than does the more delocalized bonding 5σ* orbital.

In Table IV we have compiled the measured intensity ratios of the CO 4σ level to the CO 1π + 5σ* derived level. The first column is the ratio obtained from the x-ray data and column II is the ratio from the 40.8-eV spectra. The data in column II show that for most of the carbonyls the in-

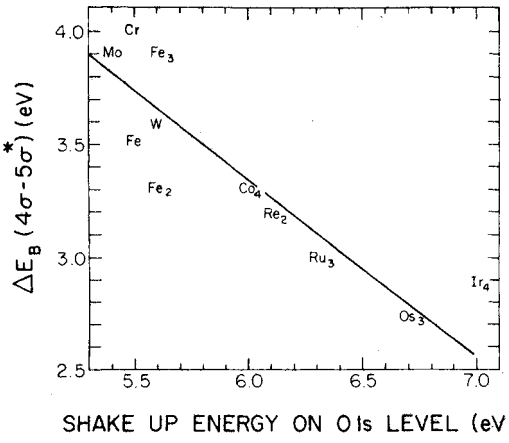

FIG. 9. Energy separation of the CO 4σ level and the bonding 5σ* level in the carbonyl complexes as a function of the observed shake-up energy on the O-1s level.

TABLE IV. Intensity ratios for valence levels $4\sigma/1\pi + 5\sigma^*$).

Carbonyl	I x ray	II uv $\hbar\omega = 40.8$ eV
CO	1.7	0.35
$Cr(CO)_6$	1.4	0.38
$Mo(CO)_6$	1.0	0.40
$W(CO)_6$	0.90	0.39
$Fe(CO)_5$	1.4	0.31
$Fe_2(CO)_9$	1.0	0.30 ± 0.02
$Re_2(CO)_{10}$	1.0	0.24
$Co_2(CO)_8$		0.38
$Fe_3(CO)_{12}$	1.1 ± 0.1	0.33
$Ru_3(CO)_{12}$	1.1	0.35
$Os_3(CO)_{12}$	1.2	0.26 ± 0.01
$Ir_4(CO)_{12}$	1.1	0.22
$Co_4(CO)_{12}$	1.4	0.33

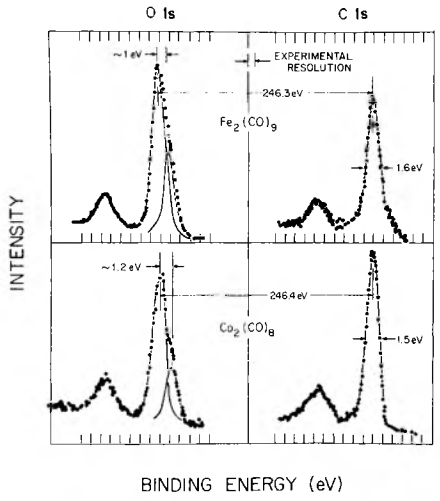

FIG. 10. C-1*s* and O-1*s* spectra of two carbonyl complexes containing bridge-bonded CO molecules.

tensity ratio is nearly the same as for gas-phase CO (first row). The x-ray ratios, however, are consistently lower than the free-CO ratio. The simplest explanation of this observation is that there is metal *d* character mixed into the $1\pi + 5\sigma^*$ orbital. The relative intensity of the emission from the *d*-metal electrons can be measured from the x-ray photoelectron spectra of the carbonyls.[24] If we calculate the percent of *d* character that would have to be mixed into the $1\pi + 5\sigma^*$ level to produce the measured ratio, we obtain ~0.2 of an electron for $Cr(CO)_6$, $Mo(CO)_6$, $W(CO)_6$. This seems to be a consistent picture for these three carbonyls since the intensity from the 5*d*'s in $W(CO)_6$ is greater than from the 4*d*'s in $Mo(CO)_6$, which are more intense than in 3*d*'s in $Cr(CO)_6$. The ratios of intensities (column I of Table IV) are consistent with this trend, i.e., the 3*d* transition-metal carbonyls usually have a larger ratio than the 4*d* or 5*d* TM carbonyls. The other abnormality shown in Table IV is the low ratio of intensity for $Re_2(CO)_{10}$, $Os_3(CO)_{12}$, and $Ir_4(CO)_{12}$ in the 40.8-eV spectra. We propose no explanation of this effect, but we will show that the same behavior exists for CO adsorbed on Ir.

E. Bridge versus terminally bonded CO

$Co_2(CO)_8$ was the only carbonyl complex that we studied which showed a resolvable splitting in a core level due to bridge-bonded CO. Figure 10 displays on the bottom the core-level spectra obtained from condensed $Co_2(CO)_8$ using Al $K\alpha$ radiation and a crystal monochromator. The O 1*s* level shows a peak of the correct intensity shifted by ~1.2 eV from the terminally bonded CO, O-1*s* peak. There was no observable splitting on the C-1*s* spectrum. Figure 10 also shows the equivalent spectra for $Fe_2(CO)_9$. The O-1*s* peak is abnormally broad and we have drawn in a possible deconvolution of this peak, giving a separation of ~1.0 eV for the O-1*s* binding energy between bridge- and terminally-bonded CO. We did not observe any abnormal line shape for the O-1*s* and C-1*s* lines in $Fe_3(CO)_{12}$. The linewidth of the C-1*s* and O-1*s* spectra was always 1.3–1.6 eV for condensed-phase carbonyls even with a instrumental resolution of 0.75 eV or less. Therefore, these splittings may only be observable for gas-phase carbonyls. Our limited data indicate the splittings are small, but are larger for the O 1*s* level than for the C 1*s* level. The binding energy of the O 1*s* level in the bridge-bonded configuration is less than in the terminal configuration.

Broden *et al.*[25] have suggested that the effects of bridge bonding should be observable in the valence spectra of carbonyls. The argument is that the carbon-to-oxygen spacing will increase in a bridge site compared to a terminal site. The effect of this increased spacing will be to increase the energy spacing between the 4σ and 1π energy levels of CO. Several theoretical papers have calculated this increased energy spacing to be about 10 eV/Å.[26] If we apply this number to the spacings given in Table I for $Co_2(CO)_8$, we would expect to see the 4σ to 1π spacing increase with respect to free CO by 0.4 eV for the terminally bonded CO and 0.7 eV for the bridge-bonded CO (see Appendix D). The number we obtain for $Co_2(CO)_8$ is 3.2 eV. Figure 8 shows that the 4σ to 1π spacing in all of the carbonyls is slightly larger than the equivalent spacing in CO; therefore, we cannot safely

conclude from our data that there is a measureable effect associated with bridge bonding (Appendix D).

F. Auger spectra

Figure 11 shows our data for the O-1*s* Auger spectrum from CO and gas- and condensed-phase $Cr(CO)_6$. The solid curve drawn through the CO data is the CO Auger spectrum obtained by Moddeman *et al.*[27] using electron excitation. The shifts in the Auger spectra are much larger than the shifts in the one-electron binding energies. For example, the O-1*s* binding energy only shifts by 3.2 eV between gas-phase CO and gas-phase $Cr(CO)_6$, while the Auger spectra shifts ~10 eV. Likewise the shift in the O-1*s* binding energy between gas- and condensed-phase $Cr(CO)_6$ is ~0.6 eV (Table II) while the Auger spectra shifts by 2.3 eV. This is clearly a result of the difference between a double (Auger)- and single (XPS)-hole final state.

The Auger process involves three hole states, the initial-hole state i and the two states j and k from which one electron drops down to fill the ith hole and the other is ejected. The kinetic energy of the ejected electron is given by

$$E_{\mathrm{K.E.}}(i,j,k) = E_{\mathrm{B.E.}}(i) - E^{\dagger}_{\mathrm{B.E.}}(j,k)\,. \tag{3}$$

where $E_{\mathrm{B.E.}}(i)$ is the measured binding energy of the initial-hole state and $E^{\dagger}_{\mathrm{B.E.}}(j,k)$ is the double-hole (j,k) ionization energy. Clearly $\Delta E^{\dagger}_{\mathrm{B.E.}}(j,k)$ between CO and $Cr(CO)_6$ must be much larger than $\Delta E_{\mathrm{B.E.}}(i)$ in order to account for the large shifts in the kinetic energy of the ejected Auger electrons. The changes observed between gas- and condensed-phase $Cr(CO)_6$ are particularly easy to understand using Eq. (3). The data in Table II shows that there is a rigid shift of all of the one electron binding energies as $Cr(CO)_6$ is condensed. Using the measured shift in the one-electron levels and Auger spectra we obtain a shift in the two electron binding energy $E^{\dagger}_{\mathrm{B.E.}}$ in Eq. (3) of 2.9 eV compared to the single-electron binding-energy shift of 0.6 eV. Within the accuracy of these measurements this produces a double-hole relaxation energy four times as large as the single-hole relaxation; the number expected from linear response.

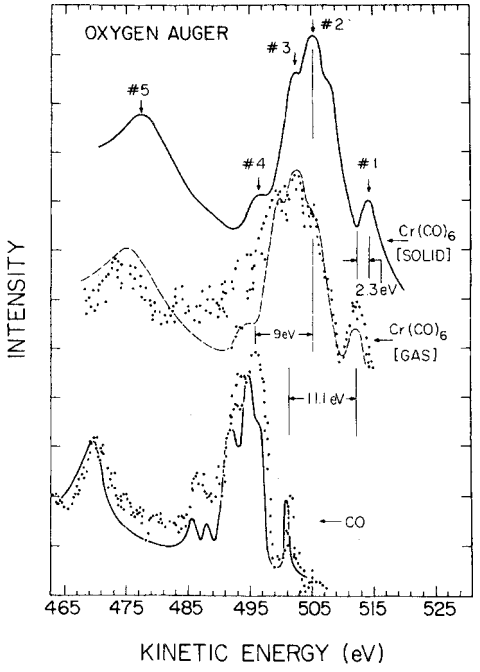

FIG. 11. Comparison of the O-1*s* Auger spectra for gas phase CO and $Cr(CO)_6$ with condensed phase Cr $(CO)_6$. The solid curve drawn through the CO data is the electron-induced Auger spectra of gaseous CO of Moddeman *et al.* (Ref. 27). The dashed curve drawn through the gas phase $Cr(CO)_6$ spectrum is the condensed phase $Cr(CO)_6$ spectrum shifted by 2.3 eV.

The O-1*s* Auger spectrum from a carbonyl exhibits basically the same features as the gas-phase CO Auger spectrum (Fig. 11). The only noticeable difference, besides the shift to higher kinetic energy, is a decrease in intensity coupled with a relative shift of peak No. 1 (Fig. 11) to higher kinetic energy as more metal atoms are added to the carbonyl complex. On the other hand, the C-1*s* Auger spectrum from a carbonyl looks quite different than the corresponding CO spectrum. Figure 12 compares our data for gas-phase CO with condensed-phase $Cr(CO)_6$. The solid line at the top is the gas-phase CO spectrum shifted by 9 eV, which is the energy shift of the main lines in the O-1*s* Auger spectrum. The dashed curve is the N-1*s* Auger spectrum from NO taken from the data of Moddeman *et al.*[27] and shifted by 100 eV.

The C-1*s* Auger spectrum from a carbonyl should differ from the gas-phase CO Auger spectrum for several reasons. First, the 5σ level is shifted considerably upon bonding. Second, the screening model we proposed for the shake-up satellites in the C-1*s* spectrum implies the occupancy of the CO 2π derived levels in the ionic state. This state should appear in the Auger spectrum. Figure 3 shows that both the 5σ and 2π orbitals are primarily centered on the carbon atom and therefore transitions involving these levels should be very intense in the C-1*s* Auger spectrum. Moddeman *et al.*[27] assign the two major peaks in the CO C-1*s* Auger spectrum to transitions involving the 5σ level. The binding energy of the 5σ level increases by 3 eV relative to the C-1*s* energy level in $Cr(CO)_6$ (Table II), therefore, we would expect to see a smaller shift in the C-1*s* Auger spectrum

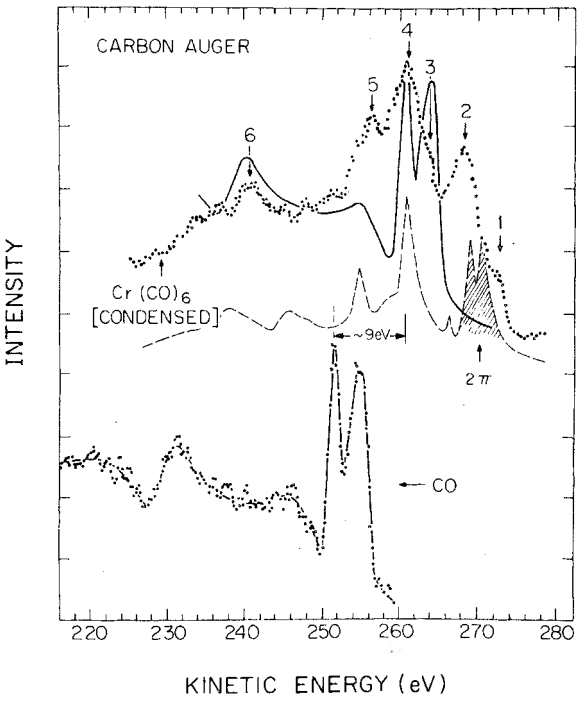

FIG. 12. C-1*s* Auger spectra from gas phase CO and condensed phase $Cr(CO)_6$. The solid curve at the top is the gas phase CO spectrum shifted by 9 eV. The dashed curve is the N-1*s* Auger spectrum of NO from Moddeman *et al.* (Ref. 27), lined up with the $Cr(CO)_6$ spectrum.

than shown in Fig. 11 for the O-1*s* Auger spectrum. It is obvious from Fig. 12 that there is a much larger shift in the highest kinetic energy peaks of the C-1*s* Auger spectrum for $Cr(CO)_6$ than there was in the O-1*s* Auger spectrum. In addition, the shape of the carbonyl spectrum is quite different than the shape of the free-CO spectrum. Peak No. 1 in the $Cr(CO)_6$ spectrum is 18 eV higher than the highest CO peak. Yet the peak labeled No. 6 in the $Cr(CO)_6$ spectrum is approximately 9 eV higher in kinetic energy than the corresponding peak in the CO spectrum. Moddeman *et al.*[27] assigned this peak to a transition which does not involve the 5σ level. Peaks 1 and 2 must originate from an energy level (or levels) whose binding energy is less than the $5\sigma^*$ binding energy. There are two possibilities: (a) there are cross Auger processes from the metal levels; or (b) these peaks originate from the 2π level which, as we explained previously, is partially filled in the process of screening the hole. There is no way of using the energies of these peaks to test either process, but the large intensity of peak No. 2 would indicate that this is not a crossed Auger process. Therefore, we believe that the C-1*s* Auger spectrum adds supporting proof to the model proposed for the screening of a core hole. The N-1*s* Auger spectrum from NO is shown in Fig. 12 by the dashed line (shifted by ~100 eV) to line up with the carbonyl spectrum.[27] The shape of the N-1*s* (NO) Auger spectrum is more similar to the C-1*s* carbonyl spectrum than is the C-1*s* CO spectrum. The shaded portions of the NO spectrum are the peaks originating from transitions involving the 2π electron.[27]

IV. COMPARISON TO ADSORBED CO

In this section we compare the features of the photoelectron spectra from the carbonyl complexes with that of CO adsorbed on a TM surface. The two adsorption systems where sufficient data are available to make such a comparison are CO on W(110),[7] and CO on Ru(001).[6] These two systems allow us to make a detailed comparison of a single-metal carbonyl $W(CO)_6$ and a multimetal carbonyl $Ru_3(CO)_{12}$ with adsorbed CO. The following sections are organized to nearly parallel the discussion of the carbonyl spectra. The individual sections will discuss shake-up, the $5\sigma^*$ binding energy, bridge bonded CO, the Auger spectra, and the numerical values of the structure in the photoelectron spectra.

A. Shake-up

Satellite structure on the O-1*s* core level of molecularly adsorbed CO has been observed for adsorption of CO on W(110),[7] and Ru(001).[6] This structure is very similar to the satellite structure observed for the carbonyls. Figure 13 shows a comparison of our data for $Ru_3(CO)_{12}$ with that of Fuggle *et al.*[6] for CO adsorbed on Ru(001). There is a 6.1-eV shift of the two binding-energy scales; ours is measured with respect to the vacuum level and Fuggle's with respect to the Ru Fermi energy. The shake-up structure is basically the same, but the energy of the main shake-up peak for $Ru_3(CO)_{12}$ is approximately 0.5 eV smaller than for the adsorption case. The difference is even more pronounced when $W(CO)_6$ is compared to the CO on W(110) data[7] (Fig. 14). The energy of the main shake-up peak for $W(CO)_6$ is 1.3 eV different than the corresponding peak in the adsorbed CO spectrum, and the two intensities are considerably different. The shake-up peak in $W(CO)_6$ is 38% of the main peak while the corresponding peak is only ~25% of the main peak for adsorbed CO.

The important observation is that the shake-up energy for CO adsorbed on W(110) is the same as the shake-up energy for CO on Ru(001), 6.9 ± 0.3 eV and 7.0 ± 0.3 eV, respectively.[7] Therefore, as we pointed out in Sec. IIA, the difference in the

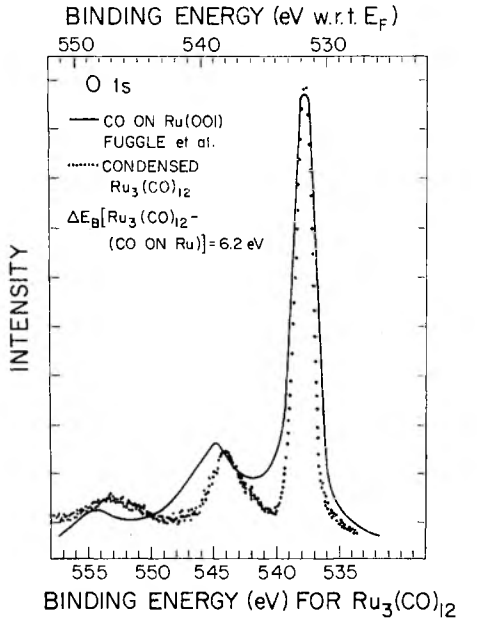

FIG. 13. O-1*s* spectra from $Ru_3(CO)_{12}$ and CO adsorbed on Ru(001) (Ref. 6). The $Ru_3(CO)_{12}$ data were obtained with a crystal monochromator and Al $K\alpha$ radiation. The binding energy of the adsorbed CO is measured with respect to the Fermi energy.

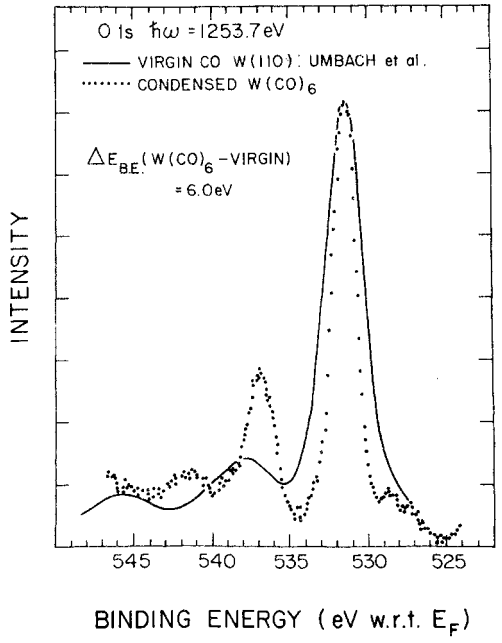

FIG. 14. O-1*s* spectra from $W(CO)_6$ and virgin CO on W(110) (Ref. 7). The carbonyl binding energy is measured with respect to the vacuum, while the absorption case is measured with respect to the Fermi energy.

shake-up energies between $W(CO)_6$ and $Ru_3(CO)_{12}$ is not a consequence of the bonding of CO but due to the size of the cluster or equivalently the delocalization of the screening hole. The W(110) and Ru(001) data are exploited in Fig. 5 to show that the carbonyl results are converging rapidly to the surface value. Within experimental error $Os_3(CO)_{12}$ and $Ir_4(CO)_{12}$ both have the same O-1*s* shake-up energy as the two adsorption systems.

The discussion above for CO adsorbed on Ru and W would indicate that for any CO adsorption system the shake-up energy on the core levels should be approximately 7 eV. This conclusion must be modified by the condition that the CO be bound to the surface with approximately the same energy as the bond energy in these carbonyls. Figure 4(b) illustrates the potential problem when CO is weakly bound to the surface or to a TM atom. In this case the shake-up energy should decrease and the intensity should dramatically increase. CO adsorbed on Cu at liquid-nitrogen temperatures is such an adsorption system. Brundle and Wandelt[28] and Norton *et al.*[29] have reported the core-level spectra for this system. These spectra are qualitatively different from the adsorption spectra shown in Figs. 13 and 14. The first satellite peak is closer to the main peak in energy and much more intense. Norton *et al.*[29] report an intensity for this shake-up 1.5 times larger than the lowest binding-energy peak (O 1*s* level), displaced 3 eV to higher binding energy. This is exactly the behavior we would have predicted from Fig. 4(b) for a weakly interacting system.

The shake-up peaks on the valence orbitals of CO are not commonly observed in a spectrum from CO adsorbed on a transition-metal surface. The data from the multimetal carbonyl complexes are consistent with this observation. The data plotted in Fig. 5 and the top of Fig. 6 show that as the shake-up energy increases the intensity observed in the valence spectra decreases rapidly. We could not observe the shake-up on the valence levels when the core-level shake-up energy exceeded ~6.5 eV. Even though the explanation of this phenomena eludes us the experimental observation on the carbonyls agrees with the observations on CO adsorbed on surfaces. There are two known exceptions where shake-up has been reported on the valence orbitals of adsorbed CO. The first is the low-temperature adsorption of CO on Cu.[31] The other example is for CO adsorbed on Pt.[30]

Conrad *et al.*[31] reported that for CO adsorbed on Cu(111) at low temperatures there was an additional peak in the valence-band photoemission spectra when compared to CO on Ni. More recent experiments on Cu(100) indicated that there may be two

additional peaks.[28,32] The explanation is straightforward, given the data on the carbonyls and the model for the shake-up intensity shown in Fig. 4. As we explained in the last paragraph, the shake-up energy is smaller for CO on Cu than for a room-temperature stable-adsorption system like CO on Ru. Therefore, we would expect that the intensity of the shake-up in the valence orbitals to be large. Allyn *et al.*[33] have used photon-dependent angle-resolved photoemission measurements to identify the energy levels for CO adsorbed on Cu(100). Their results are in agreement with this picture derived from the carbonyl data.

Miller *et al.*[30] reported the observation of a shoulder on the low kinetic energy side of the 4σ level for CO adsorbed on a Pt surface at room temperature using a photon energy of 150 eV. Our data would suggest that this wide unresolved structure is due to a different excitation process than associated with the carbonyls, such as electron-hole pair excitation.

B. $5\sigma^*$ bonding orbital

Figure 8 exhibits the energy separation between the CO 4σ level and the CO-derived $5\sigma^*$ or 1π levels for the various carbonyls as a function of the number of metal atoms in the complex. The data on the right are for CO adsorbed on different transition-metal single crystals. This latter data was obtained using two different techniques. The data for CO adsorbed on Ru(100) was obtained using the photon-energy dependence of the $5\sigma^*$ and 1π levels,[5] the same technique which we have utilized. Fuggle *et al.*[5] found that the energy separation between the 4σ and $1\pi + 5\sigma^*$ using $\hbar\omega = 40.8$ eV was 3 eV but the separation decreased by ~0.3 eV when x-rays were used. The other data shown in Fig. 8 were obtained using angular-resolved photoemission to investigate CO adsorbed on Ni(100), W(110), and Cu(100).[33,34] In all of these systems (except Cu) the $5\sigma^*$ level was found to have a higher binding energy than the 1π. Therefore, when CO bonds to a non-noble transition-metal surface the $5\sigma^*$ level drops below the 1π. This occurs for carbonyl complexes when the number of metal atoms is ≥ 4.

The case of CO adsorption on Cu(100) is anomalous both from the point of view of the experimental results themselves (compared to non-noble transition-metal adsorption) and from an analysis of the carbonyl results shown in Fig. 9. If the shake-up energy is only 3 eV, as it is for this system,[28,29] Fig. 9 would have predicted that the $5\sigma^*$ should have had a binding energy much less than the 1π, whereas Allyn *et al.*[33] have shown that the $5\sigma^*$ is nearly the same binding energy as the 1π.

TABLE V. Metal-metal spacings. Shaded regions indicate spacings which will accommodate dinuclear CO bonding.

METAL-METAL SPACINGS

Ti 2.95	V 2.61	Cr 2.5 (bcc)	Mn	Fe 2.48	Co 2.51	Ni 2.49	Cu 2.55
Zr 3.2	Nb 2.86	Mo 2.72	Tc 2.74	Ru 2.70	Rh 2.68	Pd 2.74	Ag 2.88
Hf 3.2	Ta 2.84	W 2.73	Re 2.77	Os 2.72	Ir 2.71	Pt 2.77	Au 2.88

C. Bridge vs terminally bonded

The carbonyl data showed only a small splitting in the O-1*s* energy level attributed to bridge bonding. This small splitting has not been reported for any adsorption system which might have both bridge and terminally bonded CO. Broden *et al.*[25] have proposed that the 4σ to 1π energy spacing can be utilized to determine bridge bonding. They interpreted the large (~4 eV) splitting of these two levels reported by Williams *et al.*[35] for CO adsorbed on Ni(111) as evidence for bridge bonding. More recent measurements indicate that the 4σ to 1π spacing on Ni(111) is 3.5 eV.[36] Appendix D shows data for the carbonyls which suggest that there may be a direct correlation between the C-O spacing and the energy separation of the 4σ and 1π levels, but the energy change is $\sim < 0.5$ eV.

The structural information for the carbonyls listed in Table I shows that bridge bonding occurs more frequently for clusters with small metal-metal spacing.[3] In general the metal-metal bond length should be less than 2.6 Å, with $Rh_4(CO)_{12}$ being an exception. Therefore, we compiled a list of the metals which are most likely to accommodate bridge-bonded CO. This is illustrated in the section of the periodic table shown in Table V, where the nearest-neighbor spacing is given. The cross-hatched boxes indicate the metals which could surely accommodate dinuclear bridge-bonded CO. They are primarily the 3*d* elements. The singly lined boxes indicate metals which are border-line cases (V and Rh). This table shows that it would be very unlikely to find CO bridge bonded on a tungsten surface. Yet CO could possibly be bonded on such a surface in a multinuclear site as it does in $Rh_6(CO)_{16}$.[3] Bridge bonding on a surface with larger metal-metal spacing could be induced by coadsorption or high-density CO coverages, but it should not occur in the first stages of adsorption.

D. Auger spectra

Figure 11 showed the shift in the O-1*s* Auger spectrum from CO to gas-phase $Cr(CO)_6$ and finally to condensed-phase $Cr(CO)_6$. Umbach *et al.*[7] have shown that the O-1*s* Auger spectra of CO molecularly adsorbed on W(110) and Ru(001) looks very similar in shape to the Auger spectra of gas-phase CO, but that it is shifted in energy by approximately 13 eV.[37] It is quite apparent from Fig. 11 that most of this shift in the Auger spectra is present already in a single-metal carbonyl. Figure 15 is a comparison of our Auger spectra for CO, $W(CO)_6$, and $Ru_3(CO)_{12}$ with CO on Ru(001),[6] and virgin CO on W(110).[7] The kinetic energy differences between the carbonyl spectra and that of CO adsorbed on the corresponding surface is given in Fig. 15. Most of this energy difference is due to the different zeros in the measurements, i.e., Fermi energy versus vacuum level. The difference for W is approximately 1.5 eV larger than for Ru, while the Auger spectra for CO on Ru is nearly identical to CO on W.[7] Therefore, we would, as before, conclude that the addition of more metal atoms in the molecule increased the double-hole relaxation energy compared to the single-hole relaxation energy [Eq. (3)]. This change from one to four metal atoms is small compared to the dramatic change from CO to CO bound to a singe-metal atom.

There is a noticeable change in the shape of the Auger spectra between $W(CO)_6$ and $Ru_3(CO)_{12}$ which is characteristic of the change induced by the presence of more than one TM atom in the carbonyl. The peak labeled No. 1 is not present in either one of the surface-adsorption systems or for $Ru_3(CO)_{12}$. In Appendix E we show spectra illustrating that for three metal atoms in a carbonyl complex this peak has disappeared. The peak is most likely due to a transition involving the 5σ derived orbital which, as shown in Fig.8, shifts to higher binding energy as the number of metal atoms increases.

The C-1*s* Auger spectrum from $W(CO)_6$ looks exactly like the $Cr(CO)_6$ spectra shown in Fig. 12 (Fig. 16). The kinetic energy of the peaks labeled 2, 4, and 6 in Fig. 12 for $W(CO)_6$ is 269.5, 262.3, and 244 eV. Chester *et al.*[38] have measured the C-1*s* Auger spectra of CO adsorbed on W(100). Their resolution is not as good as that shown in Fig. 12, but the energies that they obtained for these three peaks were 265, 256, and 246 eV. Given the resolution of the latter measurement

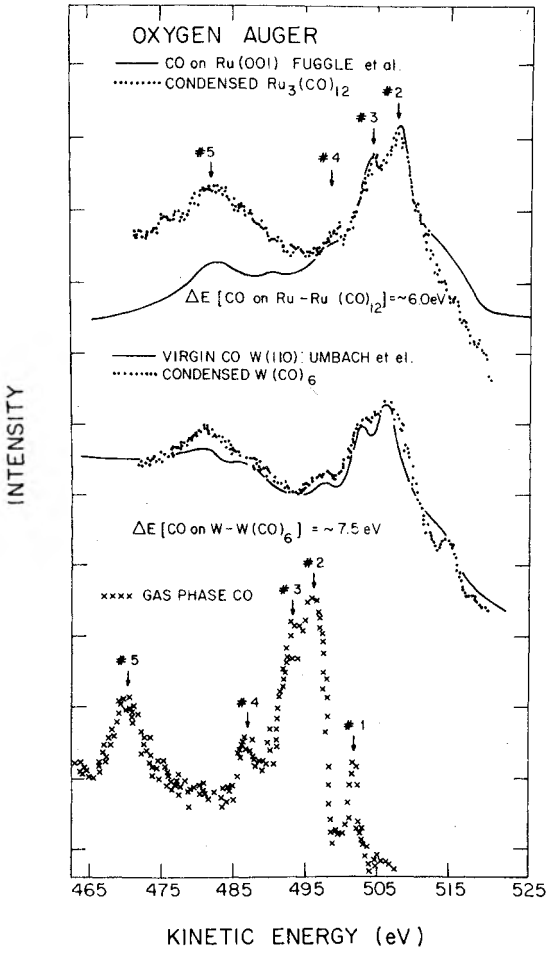

FIG. 15. O-1*s* Auger spectra from gas phase CO, condensed $W(CO)_6$ and $Ru_3(CO)_{12}$, compared to the spectra from CO on W (110) (Ref. 7) and Ru(001) (Ref. 6). The energy differences shown are between the vacuum level and the Fermi energy.

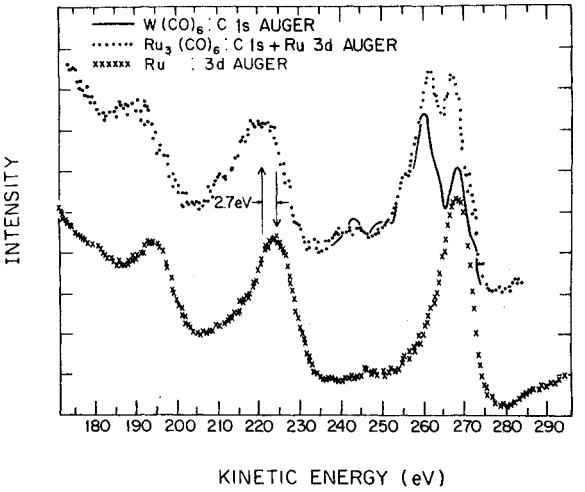

FIG. 16. Comparison of the Ru 3*d* Auger spectrum from $Ru_3(CO)_{12}$ with the spectrum from Ru.

and the different calibration of the instruments these two spectra must be considered as the same.

The C-1*s* Auger spectrum from $Ru_3(CO)_{12}$ is masked by the Ru-3*d* Auger spectrum. The combined C-1*s* and Ru-3*d* Auger spectrum is shown in Fig. 16 (top). The bottom curve is for a thin layer of Ru on a Au substrate.[39] The scales of the two spectra are fixed by aligning the Ru-3*d* photoionization peaks in the two spectra. The solid curve in this figure is the C-1*s* Auger spectrum from $W(CO)_6$. The Ru-3*d* Auger spectra are the same for both solid Ru and $Ru_3(CO)_{12}$ except for a ~3-eV shift to higher kinetic energy for the solid Ru spectrum, i.e., the screening of a double hole is more efficient in a solid piece of Ru. The correspondence between the one-electron metal-energy levels will be discussed in Sec. IV E.

E. Binding energies

The previous sections have discussed the similarities between the photoelectron spectra of TM carbonyls and CO adsorbed on a TM surface. In this section we will discuss in a more quantitative fashion the one-electron binding energies and the Auger kinetic energies for these systems. Tables VI and VII list the energies of most of the observed peaks in the photoelectron spectra for the CO-W and CO-Ru systems. These tables are separated into three sections. The upper section is the CO-derived one-electron energy levels. The middle section lists the metal levels and the bottom section compiles the O-1*s* Auger peaks. Column II of each table lists the measured energies of the respective carbonyl and column IV lists the corresponding adsorption system.

Column III of each table lists the energy shifts (where appropriate) between CO and the condensed-phase carbonyl. Both in $W(CO)_6$ and $Ru_3(CO)_{12}$ the CO-derived energy levels (top third of Tables VI and VII) exhibit a nonuniform shift with respect to their CO analog. This is the same phenomena which was discussed previously for $Cr(CO)_6$. The bottom section of column III shows that the shift

TABLE VI. Energy levels of CO and CO-W systems.

Level	I[b] CO (eV)	II[b] $W(CO)_6$ (Condensed) (eV)	III ΔE I − II (eV)	IV[c] Virgin CO on W(110) (eV)	V ΔE II − IV (eV)
1σ(O 1*s*)	542.6	537.6 ± 0.1	5.0	531.6 ±0.3	6.0 ±0.4
2σ(C 1*s*)	296.2	291.2 ± 0.1	5.0	285.5 ±0.3	5.7 ±0.4
3σ	38.3				
4σ	19.7	16.5	3.2	10.5[a] ±0.2	6.0 ±0.2
1π	16.8	~13.3[a]	3.5[a]	7.2[a] ±0.2	6.1[a] ±0.2
5σ	14.0	12.9 ~11.7[a,d]	1.1	~8[g]	~5.0
$5d$		7.1 ± 0.06		~2.5[a]	~4.6
$4f^{7/2}$		36.2 ± 0.1		30.9[e] (30.9)[f]	5.3(5.3)
$4f^{5/2}$		38.2 ± 0.15		33.0[e] (33.1)[f]	5.2(5.3)
$4d^{5/2}$		247.8		242.9[e] (242.75)[f]	4.9(5.1)
$4d^{3/2}$		260.3		255.2[e] (255.3)[f]	5.1(5.0)
$4p^{3/2}$		427.7 ± 0.2		422.7[e] (422.8)[f]	5.0(5.1)
$4p^{1/2}$		493.1 ± 0.5		487.9[e] (489.6)[f]	5.2(3.5)
O-1*s* Auger					
1	500.9	514.7 ± 0.2	−13.8		
2	494.6	506.5 ± 0.2	−11.9	513.9 ±0.5	−7.4 ±0.7
3	492	503.0 ± 0.2	−11.0	510.5 ±0.8	−7.5 ±1.0
4	486	497.7 ± 0.2	−11.7	~504	~−6
5	469.5	482.2 ± 0.5	−12.7	~487.5	~−5

[a] Data taken at $\hbar\omega = 40.8$ eV.

[b] Present data using Mg Kα radiation.

[c] See Ref. 7, measured with respect to the Fermi energy.

[d] This peak is a shoulder on the main $1\pi + 5\sigma^*$ level. It has been identified as the $8t_{1u}$ orbital (mostly 5σ) of the hexacarbonyl (Ref. 9).

[e] Measurements made by us on polycrystalline W.

[f] Measurements on W(100) by S. Semancik and P. Estrup (unpublished).

[g] Reference 33.

TABLE VII. Energy levels of CO and CO-Ru systems.

Level	I[b] CO (eV)	II[c] $Ru_3(CO)_{12}$ (eV)	III ΔE I − II (eV)	IV[d] CO on Ru(001) (eV)	V ΔE II − IV (eV)
1σ (O 1s)	542.6	537.8 ± 0.1	4.8	531.7 ± 0.2	6.1 ± 0.3
2σ (C 1s)	296.2	291.5 ± 0.1	4.7		
3σ	38.3	34.1 ± 0.3	4.2		
4σ	19.7	16.55	3.2	10.7[a]	5.9
1π	16.8	13.4[a]	3.4	7.6[a]	5.8[a]
5σ	14.0	13.5	0.5	~8.0	5.5
$4d$'s		8.05, 7.8[a]		1.9[a]	~5.9[a]
		7.25, 6.7[a]		~0.2[a]	≈6.5[a]
$4p^{3/2}$		49.3 ± 0.3		43.2 ± 0.3(43.5)[e]	6.1(5.8)
$4p^{1/2}$		51.6 ± 0.3		46.5 ± 0.5(47.7)[e]	5.1(3.9)
$3d^{5/2}$		285.8 ± 0.1		279.9 ± 0.2(279.9)[e]	5.9(5.9)
$3d^{3/2}$		289.8 ± 0.1		284.1 ± 0.2(284.1)[e]	5.7(5.7)
$3p^{3/2}$		467.0 ± 0.2		461.2 ± 0.7(461.3)[e]	5.7(5.6)
$3p^{1/2}$		489.2 ± 0.2		483.2 ± 0.4	6.0
O-1s Auger					
1	500.9				
2	494.6	507.2 ± 0.4	−12.6	514.1 ± 0.2	−6.9 ± 0.6
3	492	504.2	−12.2	510.2 ± 0.3	−6.0
4	486	498.6 ± 0.5	−12.6	505.2 ± 1.6	−6.6
5	469.5	482.3 ± 0.5	−12.8	~488.2	~−5.9

[a] Measured at $\hbar\omega = 40.8$ eV.
[b] Present data using Mg $K\alpha$ radiation.
[c] Present data using both Mg $K\alpha$ and Al $K\alpha$.
[d] See Refs. 5 and 6, measured with respect to Fermi energy.
[e] Measurements on a thin Ru film on a Au substrate.

in the O-1s Auger spectrum is slightly larger for the three-metal carbonyl $Ru_3(CO)_{12}$ than for the single-metal atom cluster $W(CO)_6$.[40] The other difference between $W(CO)_6$ and $Ru_3(CO)_{12}$ is the position of the $5\sigma^*$ level discussed in Sec. IIIC.

Column IV of both Tables VI and VII lists the CO-adsorption data.[6,7] These measurements are made with respect to the Fermi energy of the substrate metal, so that the "effective work function" of the system should be added to these data before comparing to the carbonyl data. The differences between the carbonyl and the adsorption system are listed in the last column. The CO-derived energy levels as well as the Auger spectra from CO on Ru are nearly identical to CO adsorbed on W. Therefore, the differences in column V between Tables VI and VII must reflect the size effects in the carbonyl. Within the experimental uncertainty the differences between the multimetal carbonyl $Ru_3(CO)_{12}$ and CO adsorbed on Ru(001) is 6.0 eV, for the CO levels, the metal levels, and the O-1s Auger structure.[40] There is an indication that the difference between the Ru-derived levels shown in the middle section of Table VII is slightly smaller than either the differences for the CO levels or the O-1s Auger spectra. In contrast, the data for the CO-W system in Table VI show a systematic variation in column V. First, the difference in the Auger spectra is larger in magnitude than most of the one-electron binding energies for the CO-derived levels. The second observation is that the differences in the W-derived levels (center section) are smaller than the differences in the CO levels.

Column IV of both tables indicates that the differences showing up for the W system are not a consequence of a different photoelectron spectra of CO on W compared to CO on Ru. Therefore, as emphasized, the difference in column V of Table VI for the CO-W systems is a consequence of the difference in relaxation energies between a single metal atom and a semi-infinite bulk. The data for Ru show that three metal atoms bound together are apparently as efficient at screening photoinduced single and double holes as is a semi-infinite solid. The final illustration of the similarity between the photoemission spectra of a multimetal carbonyl and adsorbed CO is shown in Fig. 17, where the

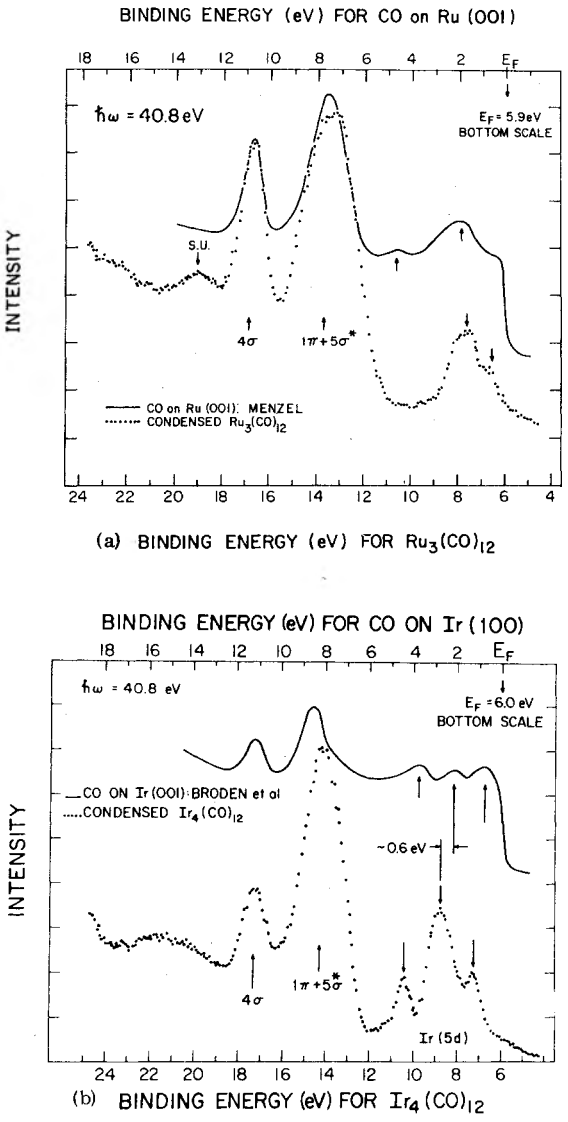

FIG. 17. Comparison of the 40.8-eV spectra of $Ru_3(CO)_{12}$ and $Ir_4(CO)_{12}$ with the spectra of CO on Ru(001) (Ref. 42) and Ir(001) (Ref. 41), respectively. The differences in the energy zero between the carbonyl and the adsorption case is the work function. S.U. in 17(a) denotes the 4σ shake-up peak.

valence-band spectra of $Ir_4(CO)_{12}$ and $Ru_3(CO)_{12}$ are compared to CO on Ir and Ru.[41,42] This figure shows that the structure in the *d* levels of the carbonyl is very similar to the band structure of the solid. Notice also that the relative intensity of the 4σ to the 1π + 5σ* for CO adsorbed on Ir is noticeably smaller than for CO adsorbed on Ru. The ratio for CO adsorbed on Ir is 25% and 38% for Ru. In Table IV we showed that this behavior was observed in the carbonyls.

Tables VI and VII do not include measurements for the binding energy of the 3σ level of CO adsorbed on the surface. Miller *et al.*[30] reported a weak peak 16.6 eV below the 4σ level for CO adsorbed on Pt, using 150-eV radiation. The energy and intensity of this peak are not consistent with our data on the carbonyls. We find, as mentioned in Sec. IIIC, that the 3σ-4σ spacing in the carbonyls is 17.8 eV, more than 1 eV larger than observed by Miller *et al.*[30] The intensity of the CO 3σ level relative to the CO 4σ level at 135-eV excitation energy is ~1.6.[43] The intensity of the peak observed on Pt was less than 30% of the 4σ intensity. Our data also indicate that there is not any abnormal change in the intensity in the x-ray spectra of the 3σ level compared to the 4σ level when CO is bound to a TM. The gas-phase ratio of intensities of these two levels at $\hbar\omega = 1254$ eV is ~2,[43] our measured value is 1.5 ± 0.3.

V. CONCLUSIONS

There are three basic conclusions of this work:

(i) More than four fifths of the shifts in the CO one- and two-electron binding energies observed when CO is adsorbed on a TM surface are present in a single-metal carbonyl. This statement applies to the energy levels not involved in the bonding.

(ii) The increased delocalization of the metal valence levels and the 5σ-derived bonding orbital in the multimetal carbonyls is sufficient to produce a photoelectron spectrum almost identical to the spectra of CO adsorbed on a surface. Three to four transition-metal atoms are required to bring both the CO and metal levels in the carbonyl into agreement with the surface system.

This conclusion should not be interpreted as total justification in treating a surface as a cluster. There are at least two reasons why some caution should be exercised. First, photoelectron spectroscopy measures the excitation spectra of an ionic system. A statement that the ionic excitation spectra of CO on a multimetal carbonyl is identical to CO adsorbed on a surface does not necessarily imply that the ground-state properties of the two systems are the same. The second point is that all of the CO molecules in a carbonyl act like a "boundary condition" for the metal cluster. We do not know that the photoelectron spectrum of one CO bound to four Ir atoms would look like $Ir_4(CO)_{12}$.

(iii) The photoelectron spectra from bridge-bonded CO are very similar to the spectra of terminally bonded CO. The O-1*s* binding energy seems to be decreased by ~1 eV compared to the C-1*s* binding energy for bridge-bonded CO. This may be a consequence of the increase in the C-O bond distance.

TABLE VIII. Binding energies of CO and gas-phase carbonyls ($\hbar\omega = 1253.7$ eV).

Level	I CO	II $Cr(CO)_6$	III ΔE (I − II)	IV $Mo(CO)_6$	V ΔE (I − IV)	VI $W(CO)_6$	VII ΔE (I − VI)	VIII $Fe(CO)_5$	IX ΔE (I − VIII)	X $Re_2(CO)_{10}$ [b]	XII ΔE (I − X)
1σ(O 1s)	542.6 eV	539.4 ± 0.1	3.2 ± 0.1	539.5 ± 0.1	3.1	539.3	3.3	539.4 ± 0.1	3.2 ± 0.1		
2σ(C 1s)	296.2	293.1 ± 0.1	3.1 ± 0.1	293.2 ± 0.1	3.0 ±	293.1	3.1	293.3 ± 0.1	2.9 ± 0.2		
3σ	38.3	35.8 ± 0.2	2.5 ± 0.3	36.5	2.8 ± 0.2					17.95 [b]	1.75
4σ	19.7	17.8	1.9(1.9) [a]	17.9	1.8(2.0) [a]	17.6	2.1(1.9) [a]			14.85 [b]	1.95
1π	16.8	{13.9}	2.9 ± 0.2	{13.9}	2.9 ± 0.2	{14.2}	2.6			13.75 [b]	−0.2
5σ	14.0		~0		~0		−0.2				
Valence										9.5	
metal										9.24	
level		8.5		8.4		8.5 ± 0.1				8.75	
										8.5	
										8.0	

[a] Data taken at 40.8 eV excitation (Ref. 24).
[b] Data taken at 40.8 eV (Ref. 44).

ACKNOWLEDGMENTS

So many people helped us during the preparation of this manuscript that they cannot all be singled out here. T. Gustafsson and D. Menzel are especially acknowledged by us for their critical and detailed reading of this manuscript. This work was partially supported by the National Science Foundation, MRL Program under Grant No. 76-00678 and by NSF Grant No. DMR 73-02656.

APPENDIX A: GAS-PHASE CARBONYLS

Table VIII lists the measured binding energies for the carbonyls that we measured in the gas phase, as well as the gas-phase CO energy levels. Columns III, V, VII, IX, and XI present the energy shifts in the respective carbonyl compared to gas-phase CO. The errors quoted in Table VIII pertain to reproducibility. We estimate from the solid-phase work that an upper limit to the error in absolute value for these binding energies is ~0.3 eV over a 600-eV energy range.

APPENDIX B: CONDENSED-PHASE CARBONYLS

Table IX presents the XPS measured binding-energy levels of the condensed-phase carbonyls which were used in this study. When there are two values given for the $1\pi + 5\sigma^*$ level, the second was measured using 40.8-eV excitation. These spectra are also shown in Appendix D. The 4σ binding energy was measured using 40.8-eV excitation and the x-ray scale calibrated by this point, therefore this table contains only the XPS and UPS measured binding energies for the $1\pi + 5\sigma^*$ level and the valence-metal levels. The bottom half of Table IX lists the binding energies of the metallic energy levels. The center row of this table gives the polarization energy, which is the reduction in the binding energy of the condensed carbonyl with respect to the gas-phase carbonyl (measured at 40.8-eV excitation).

APPENDIX C: SHAKE-UP SPECTRA

Figure 18(a) shows an expanded view of the shake-up spectra from the O-1s excitation in $Mo(CO)_6$. Figure 18(b) shows an equivalent spectrum for the C-1s spectrum of $W(CO)_6$. Table X lists the shake-up energies and relative intensities for the structure observed in the O-1s and C-1s spectra. Table XI lists the observed shake-up intensities on the valence orbitals both in the UPS and XPS data. The numbers for the $1\pi + 5\sigma^*$ level shake-up are hard to determine accurately since this peak overlaps the 4σ peak (Fig. 19 in Appendix D). The important trends are that the 4σ shake-up is always less intense in the 40.8-eV

TABLE IX. Binding energy of CO and condensed-phase carbonyls.

Level	CO [a]	$Cr(CO)_6$ [a]	$Mo(CO)_6$ [a]	$W(CO)_6$ [a]	$Fe(CO)_5$ [a]	$Fe(CO)_9$ [a]	$Re_2(CO)_{10}$
1σ (O_{1s})	542.6	538.8 ± 0.1	538.0	537.6 ± 0.1	538.1	537.7	538.1
2σ (C_{1s})	296.2	292.4 ± 0.1	291.6	291.2 ± 0.1	291.8	291.4	292.3
3σ	38.3	35.2	34.5	...	34.4	34.1	...
4σ	19.7	17.2 [c]	16.5 [c]	16.5 [c]	16.7 [c]	16.58 [c]	17.1
1π	16.8	14.0 [c]	13.5 [c]	13.3 [c]			14.0 [c]
		{13.2	{12.6	{12.9	{13.2, 13.5 [c]	{13.3, 13.2 [c]	{13.9 ± 0.2
5σ	14.0	~12.8 [c, d]	11.9 [c, c]	11.7 [c, d]			12.9 [c]
Valence					8.7 [c]	7.6 [c]	8.72 [c]
metal		7.5, 7.8 [c]	7.0, 7.1 [c]	7.1, 7.1 [c]	7.66, 8.0 [c]	7.8, 6.5 [c]	8.34, 7.67 [c]
level					6.9 [c]		~7.1 [c]
Polarization energy		0.6	~1.4	~1.2 [e]	~1.4		1.0
$5d$							
$4f^{7/2}$				36.2			46.9
$4f^{5/2}$				38.2			49.0
$5p^{3/2}$							
$5p^{1/2}$							
$4d^{5/2}$				247.8			
$4d^{3/2}$				260.3			
$4p^{3/2}$			41.8				
$4p^{1/2}$							
$4s$							
$3d^{5/2}$							
$3d^{3/2}$							
$3p^{3/2}$		50.6			51.7	51.1	
$3p^{1/2}$							
$3s$							
$2p^{3/2}$		581.5			713.7		
$2p^{1/2}$		590.4			726.2		

[a] Mg $K\alpha$ radiation.
[b] Al $K\alpha$ radiation using crystal monochromator.
[c] 40.8 eV radiation.
[d] This level is the 5σ derived $8t_{1u}$ orbital (see figure in Appendix D).
[e] Determined by shift in metal valence level.

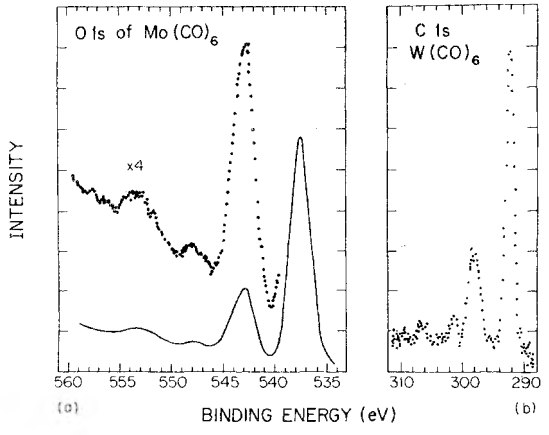

FIG. 18. (a) Expanded view of the O-1s shake-up spectra for condensed phase $Mo(CO)_6$, using Mg $K\alpha$ radiation. (b) C-1s spectra for $W(CO)_6$.

spectra than in the x-ray spectra and that the shake-up intensity decreases as the number of metal atoms in the carbonyl increases.

APPENDIX D: VUV SPECTRA

In Fig. 19 we present the 40.8-eV spectra of eight condensed TM carbonyls. The 40.8-eV spectra of $Ir_4(CO)_{12}$ and $Ru_3(CO)_{12}$ are shown in Fig. 17. Each vacuum-uv spectrum, with two exceptions, is compared to the equivalent spectrum taken using x-ray excitation: (a) the x-ray spectrum for $Cr(CO)_6$ has been shown in Fig. 7, and (b) the $Re_2(CO)_{10}$ condensed-phase spectrum is compared to the 40.8-eV spectrum of gas-phase $Re_2(CO)_{10}$.[44]

In general all of the carbonyls exhibit nearly identical spectra for the 4σ and $1\pi + 5\sigma^*$ levels.

TABLE IX (*Continued*)

$Fe_3(CO)_{12}$ [b]	$Ru_3(CO)_{12}$ [b]	$Os_3(CO)_{12}$	$Ir_3(CO)_{12}$	$Co_4(CO)_{12}$	$Co_2(CO)_{10}$
538.3 ± 0.1	537.8 ± 0.1	538.9	539.5 ± 0.2	538.3 ± 01	246.4 + C_{1s}
292.2 ± 0.1	291.5 ± 0.1	293.1	293.2	292.2 ± 02	
34.6 ± 0.2	34.1	...	34.3	34.7	
16.74	16.55	17.2	17.2	16.8	16.7
{12.74, 13.4 [c]	{13.5, 13.4 [c]	{14.45, 14.3 [c]	{14.1, 14.1 [c]	13.5 [c]	13.4 [c]
	9.25~8.6 [c]	9.71 [c]	10.3, 10.43 [c]		
7.4, 7.6 [c]	8.05 7.8 [c]	8.85, 8.61 [c]	8.3, 8.78 [c]	7.6	7.6 [c]
	7.25 6.7 [c]	7.51 [c]	7.25 [c]		
		57.0	67.2		
		59.7	70.2		
		285.0	62.0		
		299.5			
	49.3				
	51.6				
	467.0	476.5			
	489.2	554.6			
60.2	285.8				
	289.8 ± 0.1				
713.9			784.5 ± 0.1		
726.7			799.4 ± 0.1		

There are two noticeable differences. The first is that the single- and double-metal carbonyls exhibit some structure in the $1\pi + 5\sigma^*$ level. This is usually in the form of a shoulder or small peak on the low-binding-energy side of this composite peak. For the hexacarbonyls this is the $8t_{1u}$ level[9] which is a nonbonding orbital and is nearly pure 5σ in character. Notice that this peak is present in both gas-phase and condensed-phase $Re_2(CO)_{10}$. Whenever this peak is visible in the vacuum-uv spectrum it is obvious that it has much more intensity in the x-ray spectrum; see, for example, Fig. 7 for $Cr(CO)_6$ and Fig. 19 for $Mo(CO)_6$. The second noticeable difference between the spectra of different carbonyls is the change in the intensity of the shake-up peaks. We have already discussed this effect in the main text.

Conrad *et al.*[45] have compared the 40.8-eV spectrum of $Rh_6(CO)_{16}$ with the spectrum of CO adsorbed on Pd(111), concluding that the CO-derived orbitals are very similar. They indicated that this similarity demonstrated the localized character of the chemisorption bond and therefore justified the finite-cluster approximation for theoretical treatment of chemisorption. This statement is based on the implicit assumption that photoemission spectra are sensitive to the character of the chemisorption bond. Our evaluation from the data shown in Fig. 19 is that there is little information about the bond contained in these spectra except that CO is bound carbon-end down. Notice that there is no conspicuous difference between the CO-derived levels in the $Fe(CO)_5$, $Fe_2(CO)_9$, and $Fe_3(CO)_{12}$ spectra, i.e., one cannot tell bridge from terminal bonding.

Figure 20 shows an expanded comparison between the 40.8-eV spectra for $Os_2(CO)_{12}$, $Co_2(CO)_8$, and $Co_4(CO)_{12}$. These three systems were chosen be-

TABLE X. Shake-up energies and relative intensities.

Carbonyl (phase)	O 1s		C 1s	
	Energy deficit (eV)	Relative intensity	Energy deficit (eV)	Relative intensity
$Cr(CO)_6$ [a]	5.4 ± 0.1, ~ 10	0.39 ± 0.03, ~ 0.1	5.7	0.47 ± 0.03
$Cr(CO)_6$ [b]	5.5 ± 0.1, 10.0 ± 3, ~ 16.5	0.30 ± 0.02, 0.03 ± 0.1, ~ 0.07	5.7 ± 0.1, ~ 9.2	0.37 ± 0.02, ~ 0.03
$Mo(CO)_6$ [a]	5.2 ± 0.1, ~ 11.1	0.43 ± 0.03, ~ 0.12	5.6 ± 0.2	~ 0.50
$Mo(CO)_6$ [b]	5.4, 9.8, 16	0.31, 0.024, 0.06	5.7 ± 0.3	
$W(CO)_6$ [a]	5.6 ± 0.1, 10.2 ± 0.2	0.39 ± 0.02, 0.10 ± 0.02	5.5 ± 0.2, 9.0 ± 0.3	0.39 ± 0.01, ~ 0.09
$W(CO)_6$ [b]	5.6 ± 0.1, 15.7 ± 0.2	0.37 ± 0.02, ~ 0.06	5.6 ± 0.1, 8.8 ± 0.2	0.43 ± 0.02, ~ 0.10
$Fe(CO)_5$ [a]	5.7	0.29 ± 0.02	5.6 ± 0.2	~ 0.35
$Fe(CO)_5$ [b]	5.5	0.21	5.5	~ 0.22
$Fe_2(CO)_9$ [b]	5.6 ± 0.2	0.23	5.8 ± 0.2	~ 0.26
$Re_2(CO)_{10}$ [b]	6.1 ± 0.1	0.33	6.0 ± 0.1	~ 0.31
$Co_2(CO)_8$ [b]	5.4 ± 0.1	0.25 ± 0.01	5.4	0.31 ± 0.02
$Fe_3(CO)_{12}$ [b]	5.6 ± 0.2	0.23 ± 0.02	5.2 ± 0.2	~ 0.26
$Os_3(CO)_{12}$ [b]	6.7 ± 0.15	0.24 ± 0.01		
$Ru_3(CO)_{12}$ [b]	6.3 ± 0.2, 15.8 ± 0.3	0.24 ± 0.03, 0.06 ± 0.04	6.3	~ 0.28
$Co_4(CO)_{12}$ [b]	6.0 ± 0.1, 15.7	0.12 ± 0.02	5.8	0.18
$Ir_4(CO)_{12}$ [b]	7.0 ± 0.2, 15.8 ± 0.2	0.24 ± 0.01, 0.15 ± 0.02		
$Rh_6(CO)_{16}$ [c]	7.2 ± 0.4	0.08 ± 0.04		

[a] Gas phase.
[b] contlensed phase.
[c] $Rb_6(CO)_{16}$ was run on tape.

cause all of the CO's are terminally bound in $Os_3(CO)_{12}$ and the C-O spacing is 1.14 Å (Table I). On the other hand, $Co_2(CO)_8$ has two bridge-bonded CO's and the average C-O spacing is 1.18 Å, and $Co_4(CO)_{12}$ has three bridge-bonded CO's and an average C-O spacing of 1.06 Å. According to Broden *et al.*[25] the increased spacing in $Co_2(CO)_8$ should result in a 0.4-eV spacing increase between the 4σ and $1\pi + 5\sigma^*$ levels in the ultraviolet spectra. The $CO_2(CO)_8$ spectrum shows approximately a 0.3 eV larger separation between the 4σ and 1π than does $Os_3(CO)_{12}$. This is the correct direction and magnitude predicted by Broden *et al.*[25]

APPENDIX E: AUGER SPECTRA

Figure 21 shows O-1s Auger spectra for carbonyls ranging from single-metal to four-metal molecules. The spectra are basically the same except peak No. 1 which disappears as the number of metal atoms increases. Also the spectra shift

TABLE XI. Shake-up energies and intensities for valence orbitals of condensed carbonyls.

Carbonyl	4σ level at 40.8 eV (1254 eV)		$1\pi + 5\sigma^*$ level at 40.8 eV (1254 eV)	
	Energy deficit (eV)	Relative intensity	Energy deficit (eV)	Relative intensity
$Cr(CO)_6$	~ 5.2[~ 5.0]	0.12 ± 0.03[0.23]	~ 5.0[~ 5.0]	~ 0.22[~ 0.20]
$Mo(CO)_6$	5.6[~ 5.6]	0.16[0.34]	5.2[~ 5.5]	~ 0.45[~ 0.3]
$W(CO)_6$	5.4[~ 5.8]	0.10[~ 0.25]	5.3[5.6]	0.21[~ 0.2]
$Fe(CO)_5$	[~ 5.9]	[0.2]	[5.4]	[~ 0.3]
$Fe_2(CO)_9$	[~ 5.6]	~ 0.0[0.17]	5.3[ ]	0.22[ ]
$Re_2(CO)_{10}$			6.1[ ]	0.16[ ]
$Fe_3(CO)_{12}$	[~ 6.0]	[~0.25]	5.8[6.2]	0.1[0.2]
$Os_3(CO)_{12}$	[~ 6.3]	[0.05 ± 0.04]	6.8[ ]	0.09[ ]
$Ru_3(CO)_{12}$	[~ 6.0]	~ 0.0[0.0 ± 0.05]	5.8[ ]	0.06[ ]
$Ir_4(CO)_{12}$		0	0	0
$Co_4(CO)_{12}$	~ 5.9[5.9]	~ 0.06[0.18]	5.9[6.1]	0.06[0.15]
$Co_2(CO)_8$	[5.6]	[0.14]	[5.5]	[0.16]

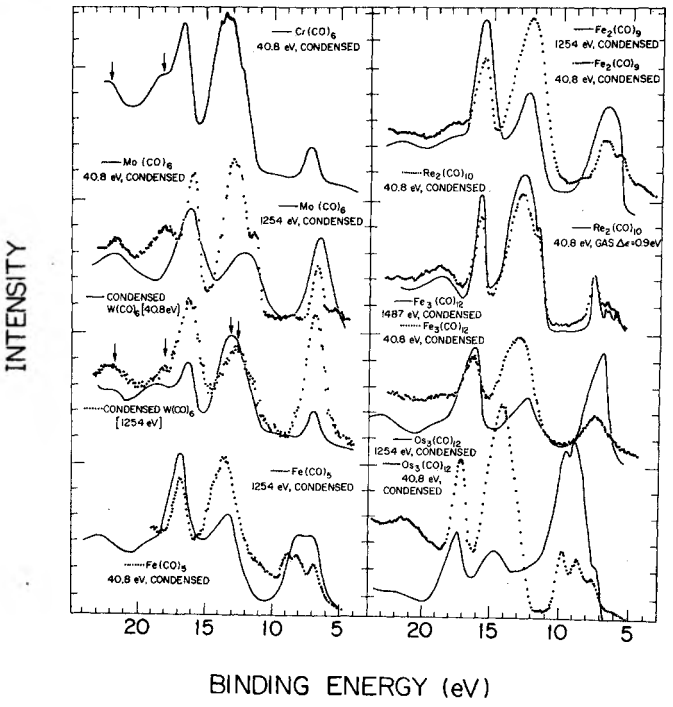

FIG. 19. Photoelectron spectra of the valence levels of eight different TM carbonyls. The 40.8-eV spectrum is shown for each carbonyl.

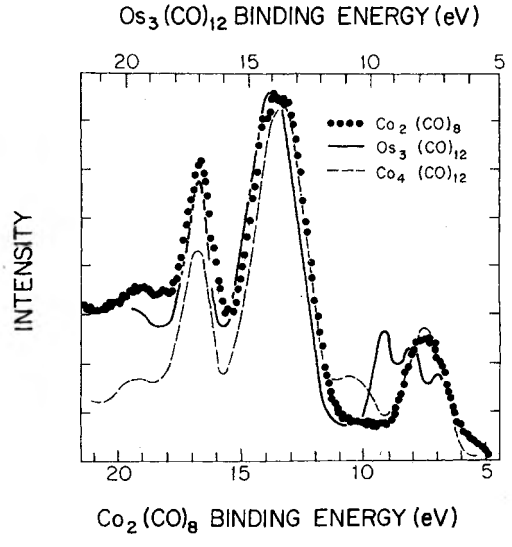

FIG. 20. Comparison of the $\hbar\omega = 40.8$-eV spectra of $Os_3(CO)_{12}$, $Co_2(CO)_8$ and $Co_4(CO)_{12}$. The spectra are aligned using the 4σ level.

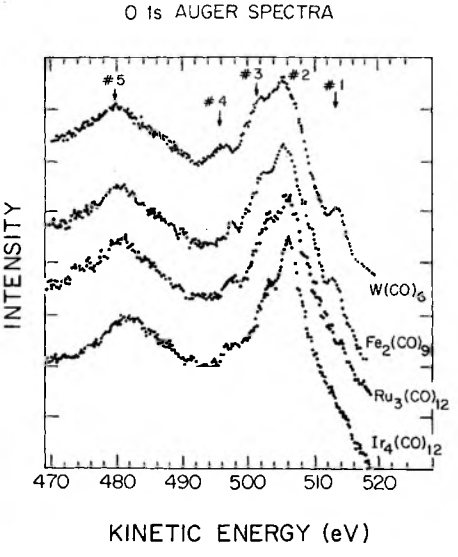

FIG. 21. O-1s Auger spectra for four different TM carbonyls.

TABLE XII. O-1*s* Auger data.

Carbonyl	Peak kinetic energy No. 1 (eV)	No. 2 (eV)	No. 3 (eV)	No. 4 (eV)	No. 5 (eV)
CO	500.9	494.6	492	486	469.5
$Cr(CO)_6$ (gas)	512.2	503.2±0.6			
$Cr(CO)_6$ (condensed)	514.5	505.4	502.1	496.3	477.6
$Mo(CO)_6$ (gas)	510.6				
$Mo(CO)_6$ (condensed)	514.5	506.2			480.7
$W(CO)_6$ (gas)	511.6	~503			
$W(CO)_6$ (condensed)	514	505.9±0.3	502.1	497	480.5

slightly (~2 eV) to higher kinetic energy. We have not listed all of the measured kinetic energies for these spectra since Tables VI and VII for $W(CO)_6$ and $Ru_3(CO)_{12}$ span the range of measured systems. Table XII lists the observed kinetic energies for the carbonyls that we could measure both in the gas and condensed phase. The energy differences in this table are used in the main text to obtain the double-hole relaxation energy for the condensed phase relative to the gas phase.

[1]E. Muetterties, Science 194, 1150 (1976); 196, 839 (1977).

[2]$Ni(CO)_4$: Spec. Publ. Chem. Soc. 11, (1958), edited by L. E. Sutton.
$Cr(CO)_6$: A. Whitaker and J. W. Jaffrey, Acta Crystallogr. 23, 977 (1967).
$Cr(CO)_6$, $Mo(CO)_6$, $W(CO)_6$: L. O. Brockway, R. V. G. Ewens, and M. W. Lister, Trans. Faraday Soc. 34, 1350 (1938).
$Fe(CO)_5$: A. Almenningen, A. Haaland, and K. Wahl, Acta Chem. Scand. 23, 224 (1969).
$Re_2(CO)_{10}$: L. F. Dahl and R. E. Rundle, J. Chem. Phys. 26, 1750 (1957).
$Fe_2(CO)_9$: F. A. Cotton and J. M. Troup, J. Chem. Soc. Dalton, Trans. 800 (1974).
$Co_2(CO)_8$: G. Sumner, H. P. Klug, and L. E. Alexander, Acta Crystallogr. 17, 732 (1964).
$Mn_2(CO)_{10}$: L. F. Dahl and R. E. Rundle, Acta. Crystallogr. 16, 419 (1963).
$Fe_3(CO)_{12}$: F. A. Cotton and J. M. Troup, J. Am. Chem. Soc. 96, 4159 (1974).
$Ru_3(CO)_{12}$: R. Mason and A. I. M. Rae, J. Chem. Soc. A, 778 (1968).
$Os_3(CO)_{12}$: E. R. Corey and L. F. Dahl, Inorgan. Chem. 1, 521 (1962).
$Ir_4(CO)_{12}$: L. F. Dahl (private communication).
$Co_4(CO)_{12}$, $Rh_4(CO)_{12}$: C. H. Wei, Inorgan. Chem. 8, 2384 (1969).
$Rh_6(CO)_{16}$: E. R. Corey, L. F. Dahl, and W. Beck, J. Am. Chem. Soc. 85, 1202 (1963).

[3]F. A. Cotton and G. Wilkinson, *Advanced Inorganic Chemistry*, 3rd ed. (Interscience, New York, 1972).

[4]J. C. Fuggle, M. Steinkilberg, and D. Menzel, Chem. Phys. 11, 307 (1975).

[5]J. C. Fuggle, T. E. Madey, M. Steinkilberg, and D. Menzel, Phys. Lett. 51A, 163 (1975).

[6]J. C. Fuggle, T. E. Madey, M. Steinkilberg, and D. Menzel, Surf. Sci. 52, 521 (1975); Chem. Phys. Lett. 33, 233 (1975).

[7]E. Umbach, J. C. Fuggle, and D. Menzel, J. Electron Spectrosc. and Relat. Phenom. 10, 15 (1977): J. C. Fuggle, E. Umbach, and D. Menzel, *Photoemission from Surfaces* (Noordwijk, 1976), p. 117. J. C. Fuggle and D. Menzel, Surf. Sci. 53, 21 (1975).

[8]D. W. Turner, C. Baker, A. D. Baker and C. R. Brundle, *Molecular Photoelectron Spectroscopy* (Wiley, New-York, 1970).

[9]J. B. Johnson and W. G. Klemperer, J. Am. Chem. Soc. 99, 7132 (1977).

[10]E. J. Baerends and P. Ros, Mol. Phys. 30, 1739 (1975).

[11]I. H. Hillier, M. F. Guest, B. R. Higginson, and D. R. Lloyd, Mol. Phys. 27, 215 (1973).

[12]T. A. Carlson, C. W. Neston, T. C. Tucker, and F. B. Malik, Phys. Rev. 169, 27 (1968).

[13]M. Barber, J. A. Conner, and I. H. Hillier, Chem. Phys. Lett. 9, 570 (1971); (see also Ref. 24); D. Rajoria, L. Kovat, E. W. Plummer, and W. R. Salaneck, Chem. Phys. Lett. 49, 64 (1977).

[14]C. E. Moore, *Atomic Energy Levels* (U. S. G.P.O., Washington, D. C., 1952), Vol. II.

[15]K. Schönhammer and O. Gunnerson, Solid State Commun. 23, 691 (1977).

[16]N. D. Lang and A. R. Williams, Phys. Rev. B 16, 2408 (1977).

[17]R. Manne and T. Åberg, Chem. Phys. Lett. 7, 282 (1970).

[18]B. I. Lundqvist, Phys. Kondens. Mater. 9, 236 (1969).

[19]E. J. Baerends and P. Ros, J. Electron Spectrosc. Relat. Phenom. 7, 69 (1975).

[20]P. S. Bagus and K. Hermann, Solid State Commun. 20, (1976); Phys. Rev. B 16, 4195 (1977).

[21]I. H. Hillier and V. R. Saunders, Mol. Phys. 22, 1025 (1971).

[22]E. J. Baerends and P. Ros, Mol. Phys. 30, 1735 (1975).

[23]D. E. Ellis, E. J. Baerends, H. Adachi and F. W. Averill, Surf. Sci. 64, 649 (1977).

[24]B. R. Higginson, D. R. Lloyd, P. Burroughs, D. M. Gibson, and A. F. Orchard, J. Chem. Soc. Faraday II, 69, 1659 (1973).
[25]G. Broden, G. Pirug, and H. P. Bonzel, Chem. Phys. Lett. 51, 250 (1977).
[26]O. Gunnerson, J. Harris, and R. O. Jones (see Ref. 25); L. S. Cederbaum, W. Dumcke, W. von Niesson, and W. Bronig, Z. Phys. B 21, 381 (1975).
[27]W. E. Moddeman, T. A. Carlson, M. O. Krause, and B. P. Pullen, J. Chem. Phys. 55, 2317 (1971).
[28]C. R. Brundle and K. Wandelt, Proceedings of the Seventh International Vacuum Congress, Vienna, 1977 (unpublished).
[29]P. R. Norton and R. L. Tapping, and J. W. Goodale, Surf. Sci. (to be published).
[30]J. H. Miller, D. T. Ling, I. Lindau, P. M. Stefan, and W. E. Spicer, Phys. Rev. Lett. 38, 1419 (1977).
[31]H. Conrad, G. Ertl, J. Küppers, and E. E. Latta, Solid State Commun. 17, 613 (1975).
[32]J. E. Demuth and D. E. Eastman, Solid State Commun. 18, 1497 (1976).
[33]C. L. Allyn, T. Gustafsson, and E. W. Plummer, Solid State Commun. 24, 531 (1977).
[34]C. L. Allyn, T. Gustafsson, and E. W. Plummer, Chem. Phys. Lett. 47, 127 (1977).
[35]P. M. Williams, P. Butcher, J. Wood, and K. Jacobs, Phys. Rev. B 14, 3215 (1976).
[36]C. L. Allyn, T. Gustafsson, and E. W. Plummer (unpublished).
[37]The data of Umbach *et al*. (Ref. 7) for CO on W(110) were referenced to the Fermi energy. They gave the shift of 19 eV.
[38]M. A. Chester, B. J. Hopkins, and R. I. Winton, Surf. Sci. 59, 46 (1976).
[39]The Ru film was formed by sputtering away the CO from the $Ru_3(CO)_{12}$ layer.
[40]The auger differences have a negative sign because they are measurements of kinetic energy instead of binding energy.
[41]G. Broden and T. N. Rhodin, Solid State Commun. 18, 105 (1976).
[42]D. Menzel, J. Vac. Sci. Technol. 12, 313 (1975).
[43]M. S. Banna and D. A. Shirley, J. Electron Spectros. Relat. Phenom. 8, 255 (1976).
[44]The gas phase $Re_2(CO)_{10}$ spectrum was furnished by D. Rajoria.
[45]H. Conrad, G. Ertl, H. Knuringer, J. Küppers, and E. E. Latta, Chem. Phys. Lett. 42, 115 (1976).